A Reevaluation of the Key Factors That Influence Tomato Fruit Softening and Integrity[1][W][OA]

Montserrat Saladié, Antonio J. Matas, Tal Isaacson, Matthew A. Jenks, S. Mark Goodwin, Karl J. Niklas, Ren Xiaolin, John M. Labavitch, Kenneth A. Shackel, Alisdair R. Fernie, Anna Lytovchenko, Malcolm A. O'Neill, Chris B. Watkins, and Jocelyn K.C. Rose*

Department of Plant Biology (M.S., A.J.M., T.I., K.J.N., J.K.C.R.) and Department of Horticulture (C.B.W.), Cornell University, Ithaca, New York 14853; Department of Horticulture and Landscape Architecture, Purdue University, West Lafayette, Indiana 47907 (M.A.J., S.M.G.); College of Horticulture, Northwest Agricultural & Forestry University, Yangling, Shaanxi 712100, China (R.X.); Department of Plant Sciences, University of California, Davis, California 95616 (J.M.L., K.A.S.); Max-Planck-Institut für Molekulare Pflanzenphysiologie, 14476 Potsdam-Golm, Germany (A.R.F., A.L.); and Complex Carbohydrate Research Center and Department of Biochemistry and Molecular Biology, University of Georgia, Athens, Georgia 30602 (M.A.O.)

The softening of fleshy fruits, such as tomato (*Solanum lycopersicum*), during ripening is generally reported to result principally from disassembly of the primary cell wall and middle lamella. However, unsuccessful attempts to prolong fruit firmness by suppressing the expression of a range of wall-modifying proteins in transgenic tomato fruits do not support such a simple model. 'Delayed Fruit Deterioration' (DFD) is a previously unreported tomato cultivar that provides a unique opportunity to assess the contribution of wall metabolism to fruit firmness, since DFD fruits exhibit minimal softening but undergo otherwise normal ripening, unlike all known nonsoftening tomato mutants reported to date. Wall disassembly, reduced intercellular adhesion, and the expression of genes associated with wall degradation were similar in DFD fruit and those of the normally softening 'Ailsa Craig'. However, ripening DFD fruit showed minimal transpirational water loss and substantially elevated cellular turgor. This allowed an evaluation of the relative contribution and timing of wall disassembly and water loss to fruit softening, which suggested that both processes have a critical influence. Biochemical and biomechanical analyses identified several unusual features of DFD cuticles and the data indicate that, as with wall metabolism, changes in cuticle composition and architecture are an integral and regulated part of the ripening program. A model is proposed in which the cuticle affects the softening of intact tomato fruit both directly, by providing a physical support, and indirectly, by regulating water status.

The ripening of fleshy fruits involves many physiological processes, including the production of aromatic compounds and nutrients, changes in color, and softening of the flesh to an edible texture, which have evolved to attract animals and promote seed dispersal (Giovannoni, 2004). The molecular pathways that underlie many of these ripening-related phenomena have been sufficiently characterized to allow the modification of fruit nutritional status or organoleptic characteristics through targeted genetic engineering (Romer et al., 2000; Lewinsohn et al., 2001; Muir et al., 2001; Dharmapuri et al., 2002; Fraser and Bramley, 2004; Davuluri et al., 2005). However, much less is known about the critical molecular determinants of fruit firmness and softening. In part, this reflects the difficulties in evaluating the many physical and sensory attributes that determine texture (Harker et al., 1997; Waldron et al., 2003), a characteristic that, unlike color or aroma, cannot be defined by a quantitative measurement of specific metabolites or by monitoring a particular biosynthetic pathway.

Research spanning more than 40 years has targeted the causal mechanisms of fruit softening, much of it using tomato (*Solanum lycopersicum*) ripening as a model system. A decline in fruit firmness typically coincides with dissolution of the middle lamella, resulting in a reduction in intercellular adhesion, depolymerization, and solubilization of hemicellulosic and pectic cell wall polysaccharides and, in some cases, wall swelling (Brummell and Harpster, 2001). These events are accompanied by the increased expression of numerous cell wall degrading enzymes, including

[1] This work was supported by the National Research Initiative of the U.S. Department of Agriculture Cooperative State Research, Education and Extension Service (grant no. 2006–35304–17323), by the Cornell University Agricultural Experiment Station Hatch Project (grant no. NYC–184485), and by the U.S.-Israel Binational Science Foundation Award (no. 2005168). In addition, A.J.M. was supported by a Ministerio de Educación y Ciencia/Fulbright (Spain) postdoctoral fellowship award and T.I. was supported by a Vaadia-BARD postdoctoral fellowship award (no. FI–375–05) from the U.S.-Israel Binational Agricultural Research and Development Fund.

* Corresponding author; e-mail jr286@cornell.edu; fax 607–255–5407.

The author responsible for distribution of materials integral to the findings presented in this article in accordance with the policy described in the Instructions for Authors (www.plantphysiol.org) is: Jocelyn K.C. Rose (jr286@cornell.edu).

[W] The online version of this article contains Web-only data.

[OA] Open Access articles can be viewed online without a subscription.

www.plantphysiol.org/cgi/doi/10.1104/pp.107.097477

polysaccharide hydrolases, transglycosylases, lyases, and other wall loosening proteins, such as expansin (Harker et al., 1997; Rose et al., 2003; Brummell, 2006). Accordingly, while factors such as cellular turgor and morphology (Lin and Pitt, 1986; Shackel et al., 1991) have been suggested to contribute to aspects of texture, mechanistic models almost invariably attribute fruit softening to disassembly of polysaccharide networks in the primary wall and middle lamella (Rose et al., 2003; Brummell, 2006). For example, polygalacturonase (PG)-catalyzed depolymerization of pectin in the wall and middle lamella was long believed to be the principal process underlying fruit softening, although this was refuted through reverse genetics studies in tomato (for review, see Brummell and Harpster, 2001). Similarly, suppressing the expression of several other ripening-related wall-modifying proteins in transgenic tomato fruits has generally resulted in minimal effects on fruit softening or texture (Brummell and Harpster, 2001; Rose et al., 2003).

Explanations for the lack of progress in identifying the key individual determinants of fruit softening include the possibility that important textural changes associated with wall disassembly are a consequence of numerous enzymes acting in concert on multiple wall structural components, or that the critical enzymatic activity or activities have not yet been identified. However, an alternative explanation is that polysaccharide degradation is not the sole determinant of fruit softening and that other ripening-related physiological processes also play critical roles.

We have addressed this latter hypothesis by evaluating a previously uncharacterized tomato cultivar, referred to here as 'Delayed Fruit Deterioration' (DFD), whose fruits undergo normal ripening, but remain firm and show no loss of integrity for remarkably extended periods after reaching the fully ripe stage. We report that ripening-related disassembly of the cell wall and middle lamella have similar characteristics in fruits from DFD and the normally softening 'Ailsa Craig' (AC), even though DFD fruits typically remain firm for at least 6 months after achieving a fully ripe stage. However, in contrast to AC fruits, those from DFD exhibit minimal water loss and consequent tissue collapse, and it is suggested that this is likely due to specific compositional or ultrastructural characteristics of the fruit cuticle. Evidence is also presented that fruit cuticles from DFD and AC tomatoes undergo distinctly different changes in their biomechanical properties during ripening. Moreover, ripe DFD fruits are highly resistant to infection by opportunistic pathogens, unless the integrity of the cuticle is compromised.

Our results suggest that while changes in the polysaccharide components of the cell wall are undoubtedly important for fruit texture, equivalent alterations in cuticle architecture are also an integral element of the ripening program. The data also highlight the mechanistic distinction between a reduction in firmness, or resistance to compression, of intact fruit, and ripening-related textural changes in the pericarp tissue. Both of these phenomena could be referred to as softening, although in most reported analyses, transgenic lines with altered expression of wall-modifying proteins have been evaluated, for obvious commercial reasons, by measuring resistance of the intact fruits to compression. This study indicates that the cuticle has a previously underappreciated influence on intact tomato fruit firmness and ripening physiology, and suggests another biotechnological target to prolong fruit quality, in addition to altering polysaccharide metabolism.

RESULTS

Physiological Characterization of DFD Fruit Development and Softening

DFD is a regionalized cultivar that is grown in specific areas of southern Europe and around the Mediterranean, where it is known to exhibit dramatically delayed softening. As far as we are aware, DFD has not been described in the literature and its genetic background is unknown. Therefore, in the absence of isogenic lines containing the introgressed DFD phenotype, the AC tomato cultivar was used for comparative purposes because it exhibits relatively rapid fruit softening and has similar fruit size, shape, and overall fruit morphology to DFD (Fig. 1). DFD and AC fruit development and ripening (from approximately 10–50 d after anthesis, as shown in Fig. 1, A and B) were

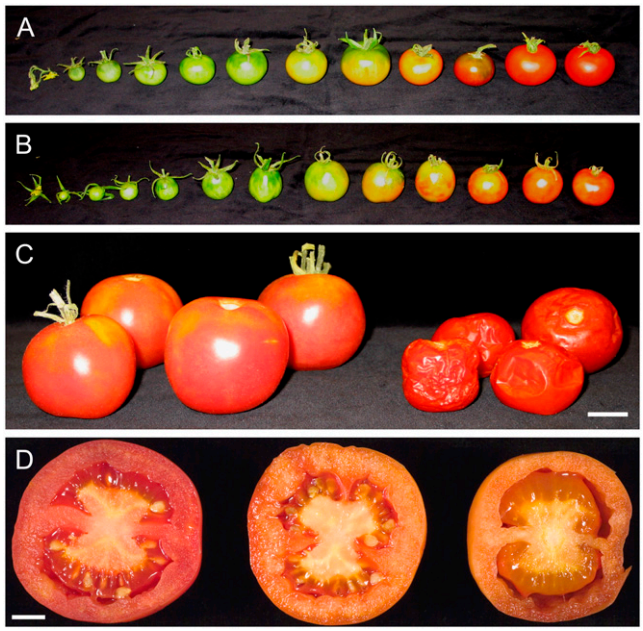

Figure 1. Comparison of AC and DFD fruit phenotypes. Developmental series of AC fruits (A) and DFD fruits (B). C, DFD (left group) and AC (right group) fruits after 4 months of storage at room temperature. Scale bar = 2 cm. D, DFD tomatoes bisected after 3 (left), 6 (middle), and 7 (right) months of storage at room temperature. Scale bar = 1 cm.

comparable, with both genotypes taking a similar time to reach a fully expanded mature green (MG) stage, although the time taken from the breaker (Br) stage, at the onset of ripening, to the red ripe (RR) stage was approximately 7 d longer for DFD than AC fruits. The peak in ethylene production showed a similar temporal delay, but the DFD fruits exhibited a characteristic climacteric respiratory burst and increase in ethylene synthesis at the Br stage (Fig. 2, A and B) that was more pronounced than that of AC fruit. This was not surprising, given the substantial variation that has been observed among tomato cultivars (Guillén et al., 2006) and was quite distinct from the suppressed climacteric in the ripening-impaired mutants *ripening inhibitor* (*rin*) and *nonripening* (*nor*; Giovannoni, 2004). Other hallmarks of normal ripening, including the accumulation of carotenoid pigments that contribute to the fruit color change (data not shown), were similar in DFD and AC, as were levels of soluble solids in the fruit, reflecting carbohydrate status (Fig. 2, C and D, respectively).

After reaching a fully ripe stage, DFD fruits remained visually unchanged for several months, as seen in photographs taken at RR plus 4 months (Fig. 1C) and a time-lapse video spanning 4 months after the RR stage (Supplemental Video S1). This was in direct contrast to AC fruits, which exhibited overripening (tissue degradation and collapse after reaching the fully ripe stage), as is typically seen in most fleshy fruits. Even 7 months after full ripening, the DFD fruits showed little change in external appearance, with no signs of internal desiccation, tissue breakdown, or other morphological changes (Fig. 1D). Storage of the fruits in the light eventually resulted in pigment photobleaching (Fig. 1D), but this did not occur in dark-stored fruits.

Compression analysis of intact AC fruits showed a typical loss of fruit firmness from MG to RR, and complete tissue collapse by 2 months after RR (Fig. 3A). In contrast, MG DFD fruits were statistically firmer than those of AC at the same stage, exhibited minimal softening during ripening, and at the RR stage were statistically firmer than AC Br fruits. Even 8 months after reaching the RR stage, the firmness of DFD fruits was similar to that of AC RR fruits. However, when the firmness of excised pericarp segments with the endocarp facing upwards was measured, no differences were seen between fruits of each cultivar at any ripening stage (Fig. 3B), although the DFD fruits were somewhat firmer at the MG stage. In contrast, the force needed to penetrate the cuticle of intact MG fruits was greater for AC than DFD (Fig. 3C), and while the AC cuticles showed progressive weakening during ripening, those of DFD showed a minimal change, such that the penetration mass for DFD fruits at the RR stage was approximately twice that of AC.

Cell Wall Analysis, Wall Disassembly, and Dissolution of the Middle Lamella

Changes in the amounts of total wall material, based on dry weight (Fig. 4A), uronic acids (Fig. 4B), cellulose (Fig. 4C), and cell wall neutral sugar composition (Fig. 4D), showed typical ripening-related trends in both AC and DFD fruits. Similarly, size exclusion chromatographic (SEC) separation of water-soluble pectins from MG and RR fruits of both cultivars showed evidence

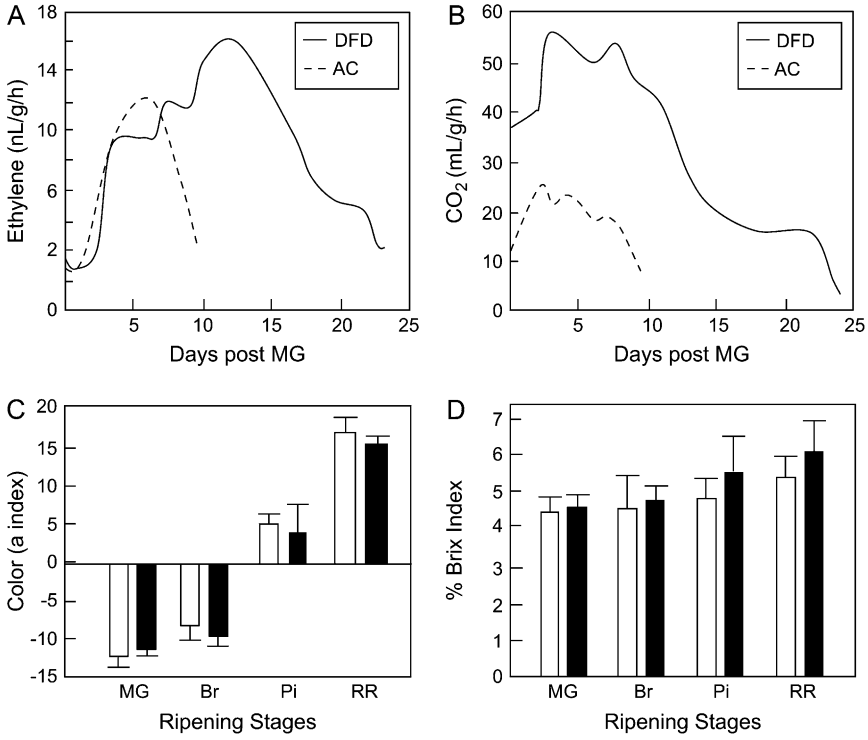

Figure 2. Ripening-related traits in AC and DFD fruits. Ethylene (A) and carbon dioxide (B) production by ripening AC and DFD fruits detached at the MG stage. C, Evaluation of external ripening-related color change of AC and DFD fruits (for C and D, mean ± SE, n = 20). D, Total soluble solids in the pericarp of AC (black bars) and DFD (white bars) fruits at the MG, Br, Pi, and RR stages, measured using a refractometer.

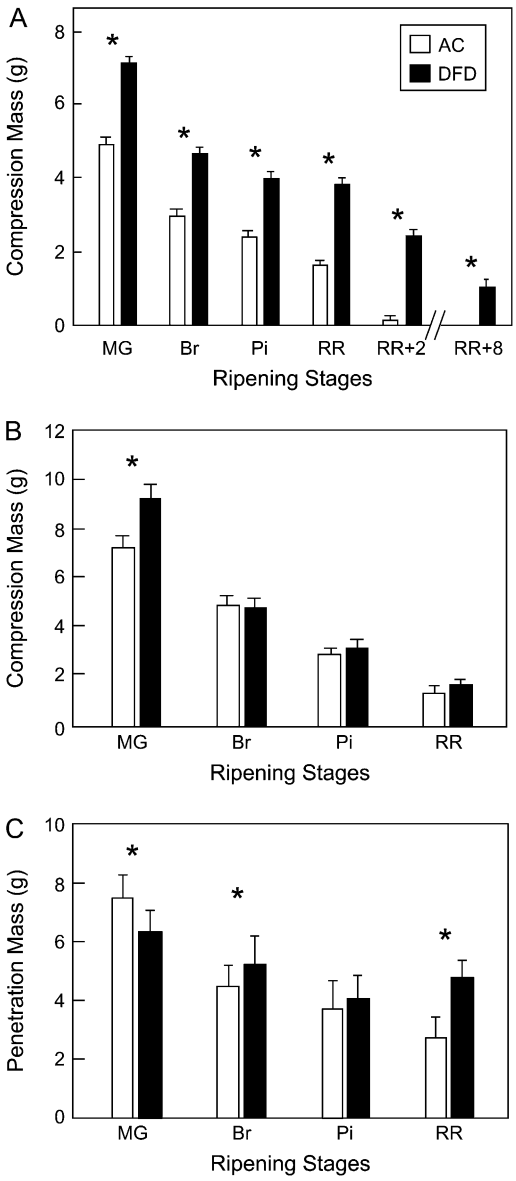

Figure 3. Textural analysis of tomato fruits. Compression test of intact tomato fruit (A) and excised pericarp segments (B). C, Penetration analysis of combined pericarp and cuticle. Fruits and pericarp segments from AC and DFD were tested at MG, Br, Pi, and RR stages and at RR plus 2 or 8 months (RR + 2 or RR + 8, respectively). Asterisks indicate statistically significance differences (mean ± SE, $n = 20$, $P < 0.001$).

of characteristic ripening-related pectin depolymerization (Fig. 4, B and E). A fractionation of chelator-soluble pectins suggested similar patterns of pectin modification in DFD and AC ripe fruits (data not shown). To further contrast ripening-related wall metabolism in the DFD and AC fruits, the expression of a range of genes encoding proteins involved in cell wall modification and disassembly, including PG, two expansins, and a xyloglucan endotransglucosylase/hydrolase, was examined by northern-blot analysis (Fig. 4F). All the genes showed similar qualitative patterns of transcript accumulation and while some quantitative differences were apparent, they were within the range of typical intercultivar variation that we have previously observed (data not shown). Importantly, the expression of these genes was not dramatically repressed, as is the case for ripening-impaired mutants such as *rin* and *nor*, where expression is generally undetectable (Maclachlan and Brady, 1994; Rose et al., 1997, 2003; Brummell and Harpster, 2001; Eriksson et al., 2004).

An examination of the fruit pericarp tissues by light microscopy (Supplemental Fig. S1, A and B) and transmission electron microscopy (TEM; Supplemental Fig. S1, C and D) showed that both AC (Supplemental Fig. S1, A and C) and DFD (Supplemental Fig. S1, B and D) ripe fruits exhibited characteristic cell-cell separation, indicating degradation of the primary wall and middle lamella and resulting in the formation of enlarged cell junction zones and cells that are interconnected only through plasmodesmata (Supplemental Fig. S1, C and D).

Pericarp Cell Swelling and Fruit Water Status

Even though fruit cell wall breakdown and cell separation showed similar trends in DFD and AC, the pericarp of DFD, but not AC, exhibited substantial swelling during ripening (Fig. 5A). Microscopic analysis of three zones of the pericarp, (1–3, corresponding to outer, middle, and inner, respectively; Fig. 5B) showed that cell size throughout the pericarp was similar in AC and DFD fruits at the MG stage (Fig. 5, B and C), but that by the RR stage, cells in the DFD pericarp had undergone a substantial increase in cell size. For example, cells in the DFD inner pericarp (zone 3; Fig. 5C) showed, on average, at least 4-fold greater increases in mean cell cross-sectional area during ripening. In contrast, while cell size in RR AC fruits was on average somewhat greater than in MG fruits, this was only statistically significant in zone 3 and the extent of the increase was far less than that seen with DFD (Fig. 5, B and C).

An increase in cell size is indicative of a positive hydrostatic (turgor) pressure that would be required to drive cell expansion. To determine whether this was the case, cellular turgor in the outer pericarp cells of AC and DFD fruits at different ripening stages was measured using a pressure microprobe (Fig. 6A, inset). Cellular turgor in AC fruits declined prior to the onset of ripening at the MG stage and decreased linearly throughout ripening, reaching minimal values at the overripe (OR) stage (Fig. 6A). The turgor values are comparable to those previously reported for other tomato cultivars (Shackel et al., 1991). The initial cellular turgor pressure and rate of linear decrease were similar in DFD fruits at the MG stage and the onset of ripening. However, in DFD, the rate of decrease slowed early in ripening and showed little further decrease after a midripe stage. An analysis of covariance indicated a significant ($P = 0.016$) difference in turgor of OR fruit between AC (0.09 MPa) and DFD (0.03 MPa) fruit, after adjustment to the same mean color level. A decline in

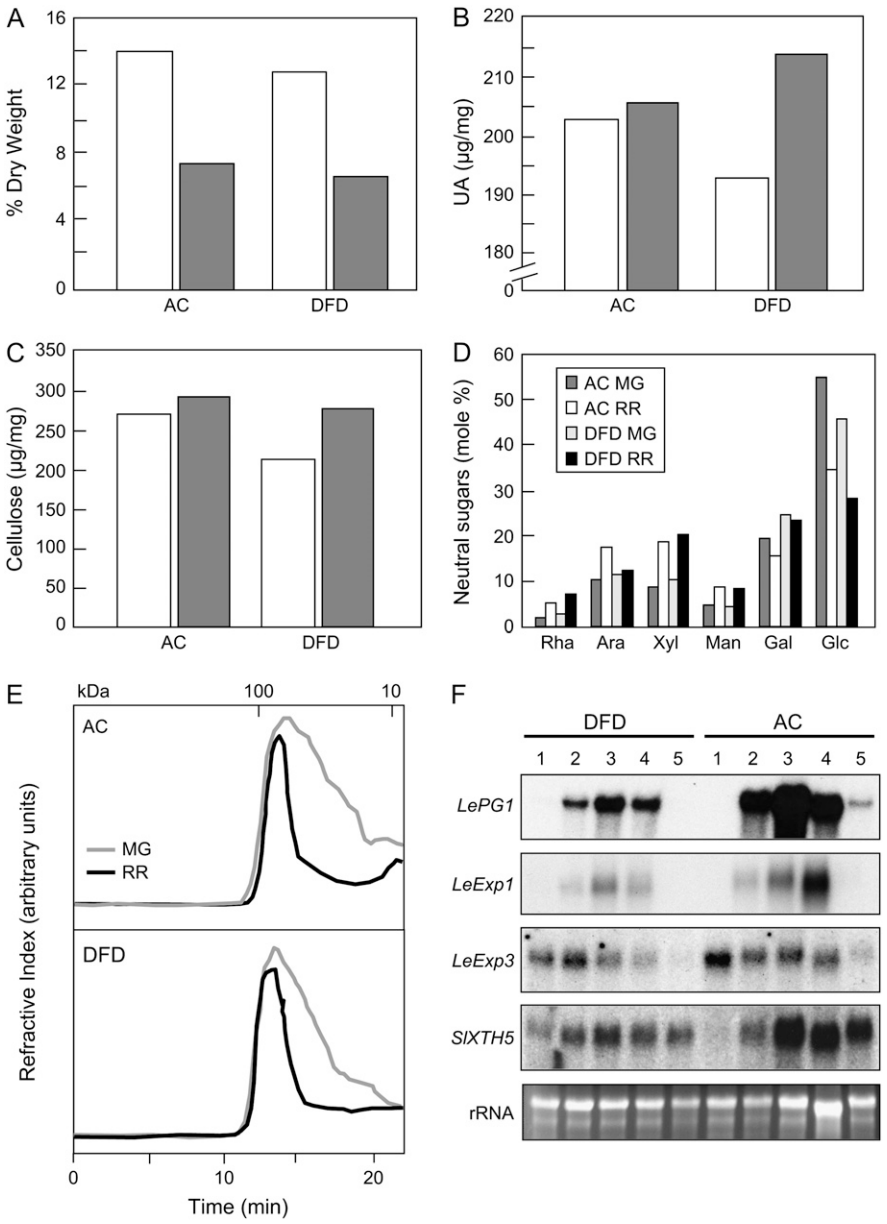

Figure 4. Cell wall analysis and wall metabolism-related gene expression. Relative amounts of cell wall pellet (A), uronic acid (UA; wall dry weight basis) content (B), cellulose content (C), and neutral sugar composition (D; mole percent of total wall noncellulosic neutral sugars) of isolated pericarp from AC and DFD fruits at the MG (white bars) and RR (gray bars) stages. For D, individual sugars comprised Rha, Ara, Xyl, Man, Gal, and Glc. E, SEC of water-soluble pectins from AC and DFD fruits at the MG and RR stages. Molecular mass calibration markers (kilodaltons) are shown at the top. F, RNA gel-blot analysis of PG (*LePG1*), expansins (*LeExp1*, *LeExp3*), and xyloglucan endotransglucosylase/hydrolase (*SlXTH5*) expression in DFD and AC pericarp. Lanes 1 to 5 correspond to the ripening stages MG, Br, Pi, RR, and OR, respectively. Ethidium bromide-stained rRNA in the same gel is shown as a loading control.

cellular turgor may be associated with water loss from the fruits, which in turn may be an important factor that contributes to the extremely delayed softening of DFD fruits. Transpirational water loss from AC and DFD fruit was assessed by measuring weight reduction over a 3 month period in fruits starting at the RR stage (Fig. 6B). AC fruits showed a high rate of water loss, while the loss was minimal in DFD fruits. After 3 months the AC fruits typically exhibited extensive desiccation and splitting, while the DFD fruits showed no apparent change, similar to the fruits shown in Figure 1C.

Microscopic Analysis of Cuticles

The cuticle provides the principal barrier to water loss in plant tissues (Jeffree, 2006) and since AC and DFD fruits exhibited substantial differences in water status, the anatomical features of their cuticles were examined by light microscopy. AC and DFD fruits have similar cuticle anatomies (Fig. 7, A–D), with substantial epidermal cell encasement, where several outer epidermal cell layers show cuticularization of the anticlinal and periclinal cell walls, as has been described in several tomato cultivars (Bargel and Neinhuis, 2004; Matas et al., 2004). Fruits of both cultivars also showed similar patterns of cellulosic cell wall ramification within the cuticular layer, as revealed by staining with toluidine blue (Fig. 7, C and D). The mean cuticle thickness of AC fruits was slightly greater ($P < 0.001$) at both the MG (12 ± 1.7 μm) and RR (11 ± 1.9 μm) stages than that of DFD cuticles (7.8 ± 1.6 μm and 8.9 ± 1.9 μm, respectively).

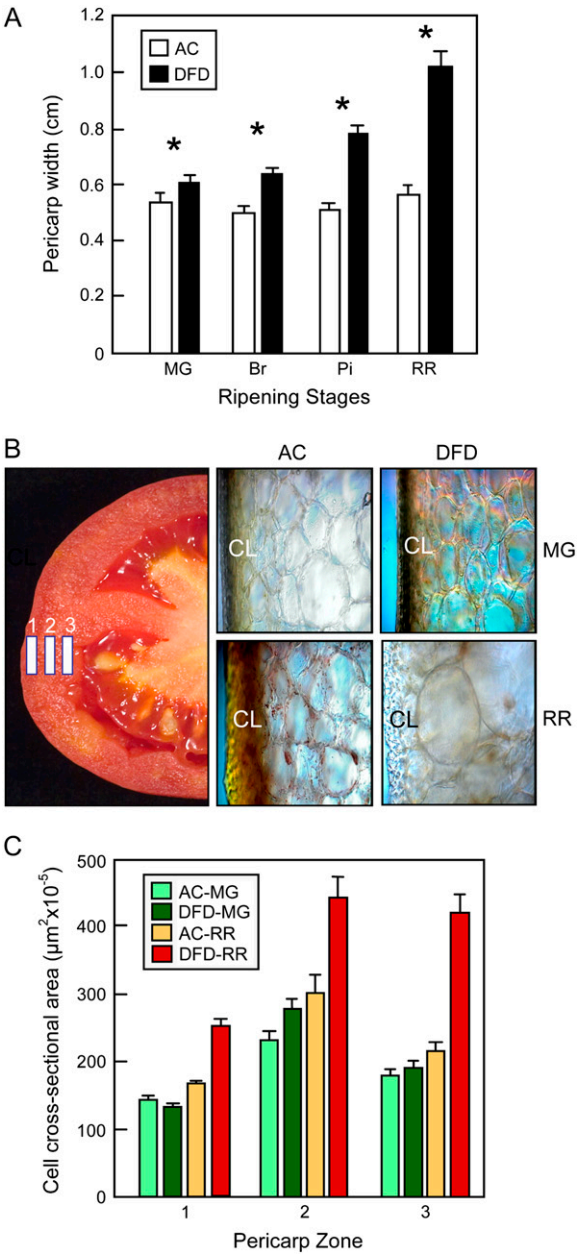

Figure 5. Pericarp and cell size measurements. A, Pericarp width of AC and DFD fruits at the MG, Br, Pi, and RR stages. Asterisks indicate statistically significance differences (mean ± SE, $n = 20$). B, Bisected RR tomato illustrating the three pericarp zones in which cell size was measured. The adjacent light microscopy photographs show cells in zone 1 and the cuticular layer (CL) from DFD and AC fruits at the MG and RR stages. C, Cell cross-sectional area in the three pericarp zones.

These values are similar to those reported for various tomato cultivars, including AC (Bargel and Neinhuis, 2004, 2005). However, one notable difference was that the cuticles of AC RR fruit had a characteristic yellow-orange color, due to the presence of the flavonoid precursor naringenin chalcone (Baker et al., 1982), but no such coloration was seen in the DFD cuticles (Fig. 7, B and D).

TEM analysis of the AC and DFD cuticles indicated no differences in ultrastructure in either the cuticular layer or periclinal and anticlinal cell walls of the outer epidermal cells (Fig. 7, E and F) and SEM imaging revealed no patterns of external wax accumulation, such as wax crystals, in either cultivar. However, during SEM analysis, focusing of the electron beam on the fruit surface consistently induced rapid peeling of a thin, outer membranous layer in the DFD samples (highlighted with an arrow in Fig. 7H), but not in AC fruits (Fig. 7G).

Analysis of Cuticle Biomechanical Properties

Enzymatically isolated cuticles from AC and DFD fruits at the MG and RR stages were evaluated with an

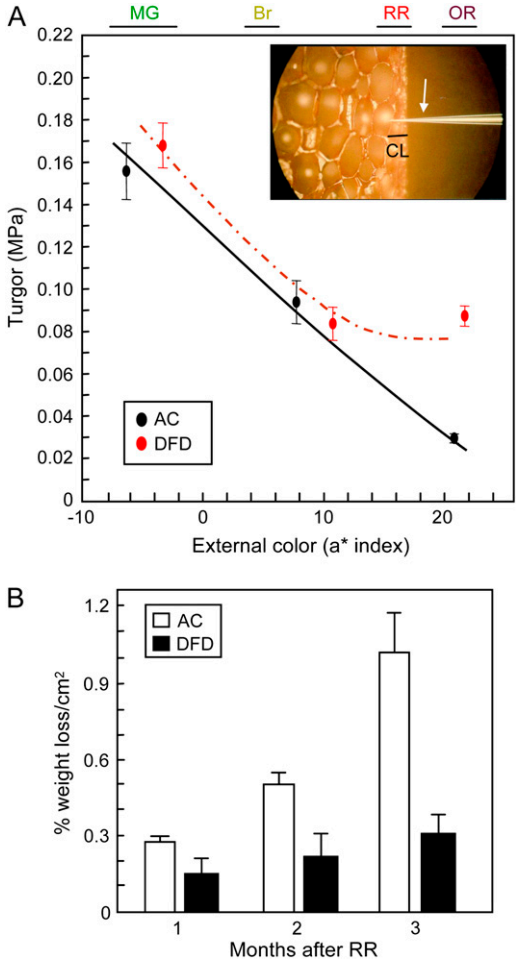

Figure 6. Pericarp cellular turgor pressure evaluation and fruit water loss. A, Turgor pressure of outer pericarp cells from AC and DFD fruits at different ripening stages, as determined by external color (a* index value). The color ranges of MG, Br, RR, and OR fruit are shown. A smoothing spline regression curve and the mean and SE (n^3 5) is shown for each cultivar. A photograph of the microprobe (white arrow) penetrating the cuticular layer (CL) and an outer pericarp cell is shown in the inset. B, Percentage water loss from detached AC and DFD fruits over a 3 month period after reaching the RR stage (mean ± SE, $n = 10$).

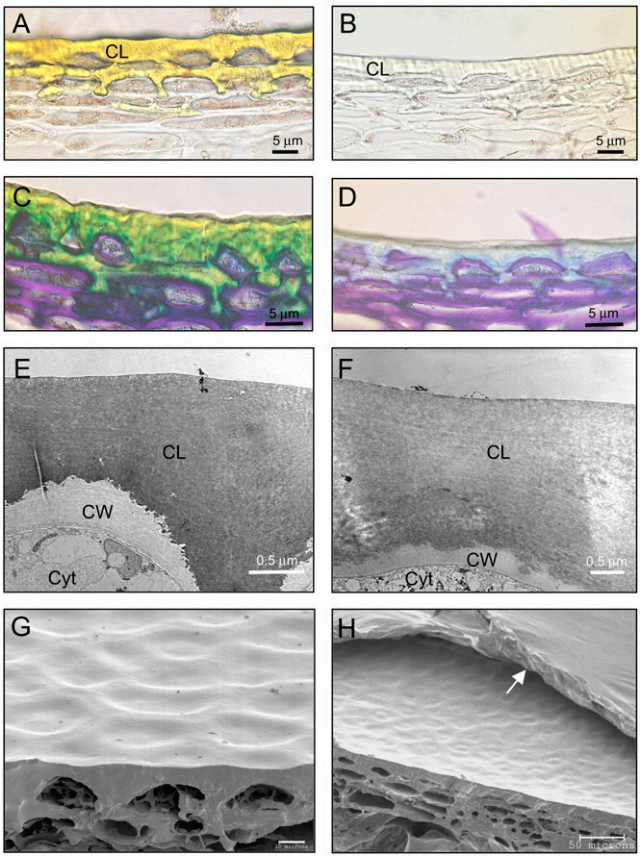

Figure 7. Microscopy analyses of AC and DFD fruit cuticles. Light microscopy images without (A and B) or with (C and D) toluidine blue O staining and TEM (E and F) and SEM (G and H) images of AC (A, C, E, and G) and DFD (B, D, F, and H) RR stage cuticles and outer pericarp. CL, Cuticular layer; CW, cell wall; cytosol, Cyt. The arrow in H indicates a thin membranous layer on the DFD fruit cuticle surface. Scale bars for A to D = 5 μm; E and F = 0.5 μm; G = 10 μm; and H = 50 μm.

Instron analyzer to determine their extensibility (strain to failure), work of fracture (energy required to induce failure), and viscoelasticity (creep rates under constant applied forces) under uniaxial loading. These tests revealed significant differences between the mechanical behaviors of the cuticles from the two cultivars, and changes in cuticle mechanical properties attending the ripening of each cultivar (Fig. 8). At the MG stage, the yield stress (i.e. the force required to induce material failure) was 33% higher in DFD than AC cuticles. Although the mean yield stress value increased during ripening in AC, there was no statistically significant change in DFD cuticles (Fig. 8A). In contrast, the AC cuticles had greater yield strains than those of DFD at the MG stage, indicating greater extensibility, and while the yield strain of AC cuticles decreased during ripening, those of DFD became markedly larger, indicating an increase in their extensibility, with a mean value approximately 30% greater than AC at the RR stage (Fig. 8B). Thus, the tensile elastic modulus E_t (i.e. the ability to resist tensile forces) of isolated cuticles differed between the two cultivars and changed during the maturation of each cultivar. At the MG stage, the E_t of DFD cuticles was significantly larger than that of AC, while at the RR stage, the E_t of AC was larger than that of DFD. Moreover, during the MG to RR transition, the E_t of AC cuticles increased, whereas that of DFD cuticles decreased. Preliminary tests to determine viscoelastic behavior (e.g. creep tests and cyclical loading-unloading tests) indicated that DFD cuticles at the RR stage deform plastically more rapidly and require smaller forces than do those of AC at the same developmental stage (data not shown).

Cuticle Composition

To determine if the cuticle chemical composition was different in AC and DFD fruits, the levels of component cuticular waxes and cutin monomers at the MG and RR stages were assayed. The total wax amount increased during ripening in both cultivars (Table I), but was higher in DFD than AC fruits at both the MG and RR stages (33% and 36%, respectively). In RR fruits, the most significant proportional differences

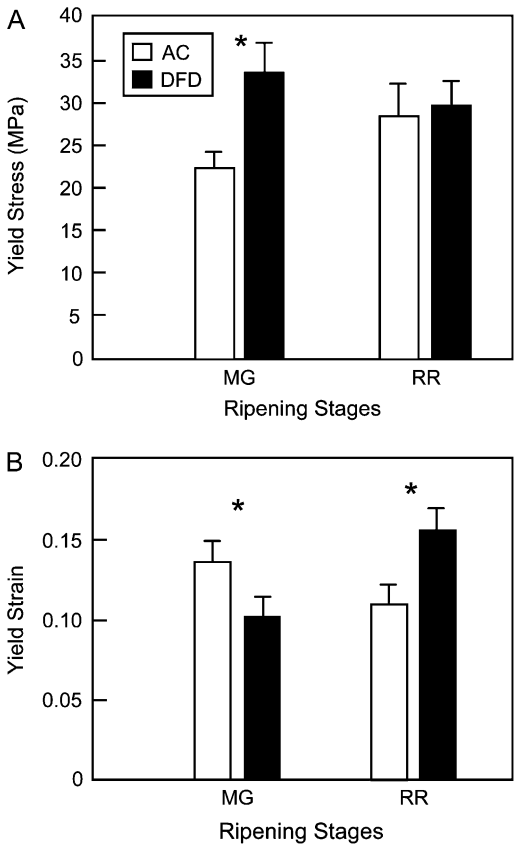

Figure 8. Instron analysis of isolated tomato fruit cuticles. The yield stress (A) and yield strain (B) of cuticles from AC and DFD fruit at the MG and RR stages, evaluated with an Instron testing machine (asterisks indicate statistically significance differences within a ripening stage; mean ± SE, n = 20).

Table I. *Wax classes in AC and DFD fruit cuticles*

Class amount (μg dm^{-2} ± SD) and class percent (% ± SD) for tomato pericarp at the MG and RR stages. Data in bold are referred to in the text.

Wax Class	MG		RR	
	AC	DFD	AC	DFD
Acids	40.7 ± 7.4	64.1 ± 13.1	36.5 ± 10.7	43.0 ± 5.8
% acids	6.7 ± 1.3	7.8 ± 0.2	4.0 ± 0.9	3.6 ± 0.4
Aldehydes	8.7 ± 2.3	11.4 ± 5.6	32.5 ± 9.5	37.5 ± 7.6
% aldehydes	1.4 ± 0.4	1.5 ± 0.9	3.5 ± 0.8	3.1 ± 0.4
n-alkan-1-ols	37.7 ± 17.5	76.9 ± 18.8	35.1 ± 5.5	53.8 ± 4.7
% *n*-alkan-1-ols	6.3 ± 3.0	9.3 ± 0.8	3.8 ± 0.3	4.5 ± 0.5
n-alkadi(tri)en-1-ols[a]	4.4 ± 3.6	5.6 ± 1.2	31.8 ± 11.8	26.5 ± 3.1
% *n*-alkadi(tri)en-1-ols	0.7 ± 0.6	0.7 ± 0.1	3.5 ± 1.1	2.2 ± 0.1
n-alkanes	336.8 ± 38.7	452.9 ± 87.4	534.2 ± 55.0	615.5 ± 63.3
% *n*-alkanes	**55.7 ± 4.8**	**55.1 ± 1.4**	**58.6 ± 1.6**	**51.1 ± 4.0**
n-alkadienes[b]	2.2 ± 0.6	2.1 ± 0.3	17.9 ± 6.0	103.9 ± 35.7
% *n*-alkadienes	**0.4 ± 0.1**	**0.3 ± 0.1**	**2.0 ± 0.8**	**8.5 ± 2.1**
iso-alkanes	34.7 ± 8.9	60.4 ± 10.0	31.9 ± 2.4	41.1 ± 9.1
% *iso*-alkanes	5.7 ± 1.3	7.5 ± 1.5	3.5 ± 0.4	3.4 ± 0.8
anteiso-alkanes	3.4 ± 1.4	3.3 ± 0.6	3.4 ± 0.5	2.2 ± 0.4
% *iso*-alkanes	0.6 ± 0.2	0.4 ± 0.1	0.4 ± 0.1	0.2 ± 0.0
Amyrins	104.9 ± 10.5	102.2 ± 12.3	159.6 ± 11.6	242.3 ± 79.7
% amyrins	17.4 ± 2.1	12.5 ± 0.8	17.6 ± 2.3	19.8 ± 4.7
Unknowns	30.6 ± 8.5	41.5 ± 14.3	27.5 ± 2.2	46.5 ± 16.6
% unknowns	5.1 ± 1.5	5.0 ± 0.9	3.0 ± 0.0	3.8 ± 0.9
Total	604.2 ± 21.1	820.5 ± 143	910.5 ± 77.4	1,212.1 ± 158.0

[a]Double bond position not determined. Position reported at $\Delta^{6,9cis}/\Delta^{3,6,9cis}$ (Bauer et al., 2004a, 2004b). [b]Double bond position not determined. Position reported at $\Delta^{6,9cis}$ (Bauer et al., 2004a, 2004b).

were apparent in the alkadienes, which showed a more than 4-fold increase in the mean percentage levels in DFD than AC, and *n*-alkanes, with lower levels in DFD (bold in Table I). Interestingly, the total and proportional amount of alkadienes increased between the MG and RR stages more than any other constituent class (Table I): In DFD fruits, the total amount of alkadienes increased nearly 50-fold from MG to RR, corresponding to a 28-fold proportional increase, while the equivalent increase in AC fruit was only 8-fold, which represents a 5-fold proportional increase. Individual wax constituents showed relatively little variation, other than substantially greater levels of tritriacontadiene in the DFD RR cuticles (bold in Table II).

Unlike the waxes, the total amounts of cutin monomers per unit fruit surface area were similar in MG and RR stages of AC fruits, but increased substantially (84%) during ripening in the DFD fruits (bold in Table III). Accordingly, while the amounts of cutin monomers were similar in AC and DFD MG fruits, the amount of cutin in DFD RR cuticles was approximately double that of AC at the same stage. The relative proportions of the monomeric constituents generally showed no significant change during ripening and no qualitative differences between AC and DFD at either ripening stage were detected. A notable exception was an increase in the proportion of 9,10,18-triOH octadecanoic acid in AC cuticles and a concomitant decrease in 9,10,18-triOH octadecenoic acid (bold in Table III). This change was not detected in DFD cuticles, which also contained higher levels of *p*-coumaric acid (Table III).

In a separate experiment, the levels of flavonoids and the flavonoid precursor naringenin chalcone were measured in total pericarp tissue minus the cuticle and outer epidermal cell layers, and in enzymatically isolated cuticles of MG and RR fruit from both cultivars. Naringenin chalcone was barely detectable in AC total pericarp extracts at the RR stage and not at all in DFD pericarp, and while levels were approximately 300-fold higher in isolated RR AC cuticles, it was not detected in DFD cuticles. The flavonoids kaempferol and quercetin were detected in MG cuticles from both cultivars and the amount of kaempferol was 2- to 3-fold greater in DFD than AC.

Infection of Fruits by Cultured and Opportunistic Fungal Pathogens

During storage and overripening it was often observed that the AC fruits became infected by opportunistic fungal pathogens, while intact DFD fruits never succumbed to infection, even following prolonged storage in high humidity conditions (Fig. 9A). To test the resistance of the DFD fruits to fungal infection in a more controlled environment, spores of the fungus *Botrytis cinerea* were applied at various titers to RR fruits from AC (Fig. 9, B and E), a commercial tomato cultivar (Fig. 9, C and F), and DFD (Fig. 9, D and G), either with a syringe through a small puncture in the fruit cuticle (Fig. 9, B–D), or ectopically

Table II. *Wax composition of AC and DFD fruit cuticles*

Individual wax constituent percentage (% ± SD) for tomato pericarp at the MG and RR stages. Data in bold are referred to in the text.

Wax Constituent	MG		RR	
	AC	DFD	AC	DFD
Acids				
Hexadecanoic acid (C_{16})	3.6 ± 1.1	4.5 ± 0.2	0.6 ± 0.3	1.3 ± 0.3
Heptadecanoic acid (C_{17})	0.1 ± 0.0	0.2 ± 0.2	0.1 ± 0.0	0.0 ± 0.0
Octadecanoic acid (C_{18})	0.5 ± 0.2	0.7 ± 0.1	0.2 ± 0.1	0.3 ± 0.2
Eicosanoic acid (C_{20})	0.1 ± 0.1	0.4 ± 0.1	0.1 ± 0.0	0.2 ± 0.1
Docosanoic acid (C_{22})	0.3 ± 0.1	0.3 ± 0.2	0.2 ± 0.2	0.0 ± 0.0
Tetracosanoic acid (C_{24})	0.2 ± 0.1	0.2 ± 0.2	1.3 ± 0.5	0.6 ± 0.4
Hexacosanic acid (C_{26})	0.2 ± 0.3	0.1 ± 0.0	0.6 ± 0.2	0.2 ± 0.1
Octacosanic acid (C_{28})	1.3 ± 0.2	0.8 ± 0.2	0.3 ± 0.1	0.5 ± 0.1
Triacontanoic acid (C_{30})	0.5 ± 0.1	0.5 ± 0.1	0.5 ± 0.1	0.4 ± 0.1
Aldehydes				
Tetracosanal (C_{24})	0.2 ± 0.2	0.2 ± 0.2	1.5 ± 0.7	0.6 ± 0.6
Hexacosanal (C_{26})	0.0 ± 0.0	0.0 ± 0.0	0.5 ± 0.1	0.1 ± 0.1
Octacosanal (C_{28})	0.0 ± 0.0	0.0 ± 0.0	0.1 ± 0.0	0.1 ± 0.0
Triacontanal (C_{30})	0.2 ± 0.2	0.4 ± 0.6	0.6 ± 0.3	1.0 ± 0.6
Dotriacontanal (C_{32})	1.0 ± 0.1	0.8 ± 0.1	0.8 ± 0.2	1.3 ± 0.3
n-alkan-1-ols				
Octadecan-1-ol (C_{18})	0.2 ± 0.2	0.1 ± 0.1	0.1 ± 0.0	0.1 ± 0.2
Eicosan-1-ol (C_{20})	0.1 ± 0.0	0.1 ± 0.1	0.2 ± 0.0	0.1 ± 0.0
Heneicosan-1-ol (C_{21})	0.0 ± 0.0	0.1 ± 0.0	0.1 ± 0.1	0.1 ± 0.0
Docosan-1-ol (C_{22})	0.2 ± 0.1	0.4 ± 0.0	0.2 ± 0.0	0.2 ± 0.1
Tricosan-1-ol (C_{23})	0.1 ± 0.1	0.1 ± 0.1	0.1 ± 0.1	0.2 ± 0.1
Tetracosan-1-ol (C_{24})	0.1 ± 0.1	0.1 ± 0.1	0.1 ± 0.1	0.1 ± 0.0
Pentacosan-1-ol (C_{25})	0.1 ± 0.1	0.1 ± 0.0	0.1 ± 0.0	0.0 ± 0.0
Hexacosan-1-ol (C_{26})	0.1 ± 0.0	0.1 ± 0.0	0.2 ± 0.0	0.1 ± 0.1
Octacosan-1-ol (C_{28})	0.2 ± 0.0	0.5 ± 0.0	0.4 ± 0.1	0.5 ± 0.2
Nonacosan-1-ol (C_{29})	0.9 ± 0.2	1.6 ± 0.1	1.3 ± 0.4	1.3 ± 0.3
Dotriacontan-1-ol (C_{32})	4.2 ± 2.9	6.1 ± 0.7	1.2 ± 0.5	1.6 ± 0.3
n-alkadi(tri)en-1-ols				
Docosadi(tri)en-1-ol (C_{22})	0.5 ± 0.4	0.5 ± 0.1	0.8 ± 0.4	0.6 ± 0.3
Tetracosadi(tri)en-1-ol (C_{24})	0.2 ± 0.2	0.2 ± 0.1	1.9 ± 0.8	0.8 ± 0.1
Hexacosadi(tri)en-1-ol (C_{26})	0.1 ± 0.0	0.0 ± 0.0	0.8 ± 0.0	0.8 ± 0.2
n-alkanes				
Tricosane (C_{23})	0.1 ± 0.0	0.4 ± 0.4	0.2 ± 0.1	0.1 ± 0.1
Tetracosane (C_{24})	0.0 ± 0.0	0.0 ± 0.0	0.1 ± 0.0	0.1 ± 0.0
Pentacosane (C_{25})	0.0 ± 0.0	0.0 ± 0.0	0.1 ± 0.0	0.0 ± 0.0
Hexacosane (C_{26})	0.3 ± 0.2	0.2 ± 0.1	0.3 ± 0.2	0.4 ± 0.2
Heptacosane (C_{27})	0.3 ± 0.0	0.5 ± 0.1	0.3 ± 0.1	0.3 ± 0.1
Octacosane (C_{28})	0.5 ± 0.1	1.1 ± 0.2	0.6 ± 0.1	0.9 ± 0.3
Nonacosane (C_{29})	8.7 ± 0.8	16.3 ± 1.0	7.5 ± 1.3	10.9 ± 3.2
Triacontane (C_{30})	5.2 ± 0.5	4.9 ± 0.4	9.4 ± 2.5	6.4 ± 2.1
Hentriacontane (C_{31})	25.4 ± 3.7	20.8 ± 3.0	29.3 ± 1.2	24.4 ± 2.6
Dotriacontane (C_{32})	3.6 ± 0.7	2.0 ± 0.4	4.5 ± 0.3	2.9 ± 1.0
Tritriacontane (C_{33})	10.3 ± 0.8	7.6 ± 2.2	4.9 ± 1.1	3.1 ± 1.5
Tetratriacontane (C_{34})	1.2 ± 0.1	1.1 ± 0.1	1.0 ± 0.1	1.1 ± 0.2
Pentatriacontane (C_{35})	0.3 ± 0.2	0.0 ± 0.0	0.4 ± 0.1	0.4 ± 0.1
n-alkadienes				
Tritriacontadiene ($C_{33:2}$)	**0.4 ± 0.1**	**0.3 ± 0.1**	**2.0 ± 0.8**	**8.5 ± 2.1**
iso-alkanes				
2-Methyl octacosane (*iso*-C_{29})	0.2 ± 0.1	0.5 ± 0.2	0.2 ± 0.1	0.4 ± 0.7
2-Methyl nonacosane (*iso*-C_{30})	0.4 ± 0.1	0.8 ± 0.2	0.3 ± 0.1	0.2 ± 0.0
2-Methyl triacontane (*iso*-C_{31})	4.2 ± 1.0	5.5 ± 1.0	2.4 ± 0.4	2.5 ± 0.3
2-Methyl hentriacontane (*iso*-C_{32})	0.8 ± 0.2	0.8 ± 0.1	0.5 ± 0.1	0.3 ± 0.1
anteiso-alkanes				
3-Methyl hentriacontane (*anteiso*-C_{32})	0.6 ± 0.2	0.4 ± 0.1	0.4 ± 0.1	0.2 ± 0.0
Amyrins				
α	5.4 ± 0.7	4.8 ± 0.3	4.5 ± 0.9	5.9 ± 1.7
β	8.2 ± 0.9	6.1 ± 0.7	5.5 ± 1.0	4.7 ± 1.5
Δ	3.7 ± 1.6	1.7 ± 0.2	7.6 ± 2.5	9.2 ± 2.4
Unknowns	5.1 ± 1.5	5.0 ± 0.9	3.8 ± 0.9	3.0 ± 0.0

(Fig. 9, E–G). Fruit from AC and the commercial tomato cultivar were consistently infected by both ectopic application and through the wound, whereas DFD fruits were only infected when the cuticle was damaged, upon which infection occurred at the same rate and to the same extent as in the other cultivars.

DISCUSSION

DFD Provides a Unique Source of Genetic Material to Dissect Fruit Softening

One of the advantages of tomato as an experimental model to study fleshy fruit softening is the availability of pleiotropic nonripening mutants, such as *rin*, *nor*, *alcobaça*, and *colorless nonripening*, which are impaired in many ripening-related processes and exhibit delayed or impaired softening (Kopeliovitch et al., 1980; Thompson et al., 1999; Orfila et al., 2002; Eriksson et al., 2004; Giovannoni, 2004). These mutants have provided insight into several specific aspects of ripening-related wall metabolism (Rose et al., 2003; Eriksson et al., 2004), but their pleiotropic nature limits characterization of more complex physiological processes. To date, to our knowledge, no tomato mutants have been characterized that exhibit minimal fruit softening, but otherwise normal ripening: such a tomato would provide an invaluable system to identify the structural and regulatory determinants of fruit firmness. We note that transgenic tomato lines with suppressed expression of the small GTPase LeRab11a were reported to have prolonged firmness, by approximately 20 d, and normal color development (Lu et al., 2001); however, no cell wall analyses were described and so direct comparisons cannot be made with the results here.

DFD fruits exhibit a substantial climacteric burst of ethylene and carbon dioxide production at the onset of ripening and undergo normal ripening, as determined by assessing color, soluble sugars (Fig. 2), metabolite content, and aroma (data not shown), in contrast to all previously reported pleiotropic tomato mutants. However, DFD fruits show remarkably small changes in their firmness when compared with the well studied experimental AC and indeed, as far as we are aware, with all previously reported tomato cultivars. While some tomato mutants show delayed softening for up to several weeks (Mutschler, 1984; Schuelter et al., 2002), DFD fruits typically remain firm for at least 6 months after reaching the RR stage, exhibiting negligible tissue collapse (Figs. 1, C and D and 3A).

The common assumption that fruit softening (applying the most commonly used definition, of resistance of intact fruits to compression) is primarily, or even exclusively, the result of wall disassembly (Brownleader et al., 1999; Brummell and Harpster, 2001; Seymour et al., 2002; Rose et al., 2003; Brummell, 2006) is challenged by the data presented here. DFD fruits remained firm at the RR stage and were significantly firmer than AC fruits at the Br and RR stages, although patterns of wall polysaccharide modification and related gene expression, and the subsequent reduction in intercellular adhesion, were comparable in DFD and AC (Fig. 3). It is noted that while the levels of LePG1 and LeExp1 transcript accumulation were somewhat lower in DFD than AC, this was within the range of variation that we have previously observed among different tomato cultivars (data not shown). Moreover, other studies have reported substantial variation among normally softening tomato cultivars of cell wall polysaccharide depolymerization, the abundance of cell wall degrading proteins and the corresponding enzyme activities (Wallner and Bloom, 1977; Carey et al., 1995; Blumer et al., 2000; Banik et al., 2001). These results indicate that the prolonged firmness of DFD fruit is not solely a consequence of impaired metabolism of the wall and middle lamella, although we cannot exclude the possibility that minor differences in wall metabolism, that were not detected in our analyses, contribute to some extent to the differences between DFD and AC softening rates. Nevertheless, it is clear that ripening-related wall metabolism in DFD is substantial, unlike previously described non-softening pleiotropic tomato mutants (Maclachlan and Brady, 1994; Rose et al., 1997, 2003; Brummell and Harpster, 2001; Eriksson et al., 2004).

DFD Fruits Show Abnormal Water Relations and Cellular Turgor

It has been suggested that fruit firmness, in common with the biomechanical properties of most plant tissues, is influenced by cellular turgor pressure (Shackel et al., 1991; Jackman et al., 1992; Jackman and Stanley, 1995; Mignani et al., 1995; Harker et al., 1997; Barrett et al., 1998). This idea has yet to be proven experimentally, but is supported by our data and other studies that have shown that ectopic application of wax to avocado (*Persea americana*) fruits can prolong their firmness (Jeong et al., 2003). Importantly, maintenance of DFD fruit firmness coincided with an absence of water loss and tissue collapse that is typical of most ripening fruits. Atypical water status in DFD fruits was also suggested by the observation that during ripening, the pericarp underwent a substantial increase in thickness (Fig. 5A), which reflected cell expansion throughout the pericarp (Fig. 5, B and C). Cell expansion requires wall loosening and a positive cellular turgor pressure (Cosgrove, 1993) and since wall degradation, which presumably resulted in a major loss in wall tensile strength, was evident in both DFD and AC RR fruits, we hypothesized that cellular turgor might be substantially different between the two cultivars. This proved to be the case (Fig. 6A) and while turgor declined during ripening in AC fruits, as has been previously reported in other normally softening tomato cultivars (Shackel et al., 1991), it remained high in DFD, after an initial decrease in early ripening. The transpiration rate from ripening tomato fruits would undoubtedly have a profound effect on tissue water status, and hence turgor pressure, but

Table III. *Cutin composition of AC and DFD fruit cuticles*

Cutin monomer acid percentages (% ± SD) for tomato pericarp at the MG and RR stages. Data in bold are referred to in the text.

Cutin Monomer	MG		RR	
	AC	DFD	AC	DFD
Hexadecanoic	0.1 ± 0.0	0.1 ± 0.0	0.1 ± 0.0	0.1 ± 0.0
16-OH hexadecanoic	3.8 ± 0.3	3.8 ± 0.7	3.2 ± 0.5	2.5 ± 0.2
10,16-DiOH hexadecanoic[a]	73.0 ± 6.3	72.0 ± 3.6	74.4 ± 2.4	74.7 ± 2.3
Hexadecane-1,16-dioic	1.3 ± 0.3	1.4 ± 0.7	1.4 ± 0.4	1.4 ± 0.6
18-OH octadecanoic	3.0 ± 1.7	2.8 ± 1.7	4.7 ± 0.8	3.1 ± 0.9
9,18-DiOH octadecanoic	1.5 ± 0.3	1.6 ± 0.5	1.4 ± 0.2	1.7 ± 0.2
9,10,18-TriOH octadecanoic	0.4 ± 0.1	0.7 ± 0.3	0.7 ± 0.1	0.6 ± 0.1
9,10,18-TriOH octadecenoic[b]	**1.4 ± 0.3**	**1.5 ± 0.6**	**0.6 ± 0.3**	**1.2 ± 0.4**
p-coumaric	0.9 ± 0.3	1.0 ± 0.1	0.6 ± 0.3	1.1 ± 0.1
m-coumaric	1.4 ± 0.6	1.5 ± 0.3	1.4 ± 0.7	1.5 ± 0.3
Unknowns	13.1 ± 5.0	13.5 ± 3.4	11.5 ± 1.5	11.9 ± 2.7
Total (μg cm^{-2} ± SD)	**1,050.4 ± 100.5**	**1,025.8 ± 196.3**	**1,102.7 ± 233.5**	**1,887.3 ± 103.6**

[a]Isomer composition: 10,16, 76%; 9,16, 10%; 8,16, 13%; 7,16, 1%. Isomer composition varied little between AC and DFD (data not shown). [b]Double bond position not determined. Position reported at Δ12 carbon (Baker et al., 1982).

another important consideration is the relative partitioning of osmotically active solutes between the symplast and apoplast. The concentration of such solutes, comprising mostly hexoses and inorganic ions (Ruan et al., 1996), increases 2-fold in the tomato fruit apoplast during ripening (Almeida and Huber, 1999), which would cause an increase in the apoplastic water potential and presumably lower cellular turgor. Such a process might explain the observation that the turgor pressure in tomato fruit pericarp cells is substantially less than would be expected, based on the osmotic potential of the entire tissue (Shackel et al., 1991). Thus, while the unusually elevated cellular turgor in ripe DFD fruits is likely to be profoundly affected by the absence of transpiration, an atypical partitioning of osmotically active solutes between the apoplast and symplast may also be a contributing factor.

DFD Cuticles Show Unusual Biomechanical and Biochemical Characteristics

The notable difference in DFD fruit water status and puncture analysis of the fruit skin (Fig. 3C) suggested an association with the cuticle, which acts as the primary barrier to transpirational water loss from aerial tissues (Riederer and Schreiber, 2001; Burghardt and Riederer, 2006) and provides a biomechanically important structure, since tensile stresses are presumably highest in the outer layer of plant tissues (Niklas, 1992). It has been reported that most gas exchange in detached tomato fruits occurs through the stem scar (Cameron and Yang, 1982; Klee, 1993) rather than the fruit cuticle. However, it was apparent that the DFD phenotype did not reflect reduced water loss through this route since sealing the stem scars of DFD or AC fruits with a layer of vaseline did not alter the relative rates of water loss (data not shown). Detached fruits also exhibited the same rate of reduction in firmness whether or not the calyx was left attached. Similarly, microscopic analysis revealed no anatomical differences in the stem scars of the two genotypes and our studies suggest that approximately equal amounts of transpirational water loss occur through the stem scar and cuticle (data not shown).

No gross differences in DFD and AC cuticle ultrastructure (Fig. 7) were seen and cuticle thickness was not statistically different between the two cultivars. This was not unexpected, since there is no correlation between cuticle thickness and water permeability in leaves (Riederer and Schreiber, 2001), or between cuticle structural appearance and water loss from blueberry (*Vaccinium* sp.) fruit (Vega et al., 1991). Light microscopy suggested no difference in the ramification of polysaccharides within the DFD and AC cuticle, which was of interest since it has been suggested that polysaccharide tracks might provide a path for water diffusion (Burghardt and Riederer, 2006).

Our data suggest that the DFD cuticle is stiffer and stronger than that of AC at the MG stage (Fig. 8). Since breaking stresses are calculated by normalizing applied mechanical forces with respect to the cross-sectional areas on which they act, the differences in breaking stresses between cultivars and developmental stages must reflect differences in the cuticle (ultra) structure or biochemical composition (Niklas, 1992). A difference in the DFD cuticle architecture was also suggested by the electron beam-induced peeling of an outer cuticular layer during SEM analysis (Fig. 7H). Cuticles are composites of a solvent-soluble wax component that is associated with a complex insoluble matrix of hydroxy- and epoxy-fatty acid esters, termed cutin (Jeffree, 2006). The waxes can be divided into two spatially distinct layers: the epicuticular waxes that coat the surface and the intracuticular waxes that are embedded in the cutin matrix. The pathways by which water diffuses through the cuticle are still poorly defined (Schreiber, 2005; Burghardt and Riederer, 2006; Schreiber, 2006) and the cuticle components that determine water permeance have not yet been identified. However, it has been suggested that long-chain saturated aliphatic hydrocarbons

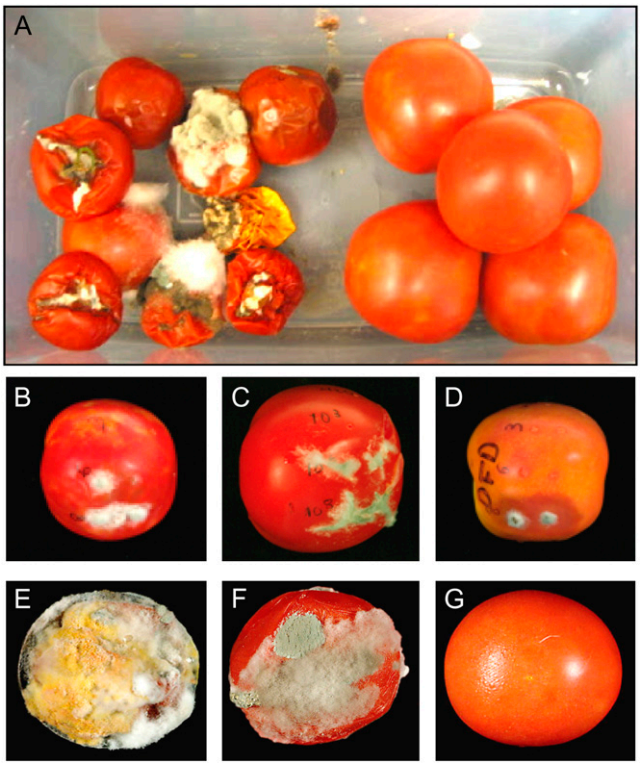

Figure 9. Microbial infection of AC and DFD fruits. A, RR fruits from AC (left side) and DFD (right side) stored for 5 months in high humidity and temperature conditions. Ripe fruits from a commercial cultivar (B and E), AC (C and F), and DFD (D and G) following inoculation with three concentrations of *B. cinerea* spores through surface penetrations (B–D) or applied ectopically (E–G).

of the intracuticular waxes, which can exhibit close molecular packing within the cutin matrix and form highly water-impermeable crystalline regions within the cuticle (Casado and Heredia, 2001), provide the principal barrier to water loss (Riederer and Schreiber, 2001; Burghardt and Riederer, 2006).

MG and RR DFD fruit have approximately 30% more wax than AC and a substantially increased level of *n*-alkadienes at the RR stage, which are inferred to be *n*-tritricontadiene (*n*-C_{33}-6,9-diene) from previous analyses (Bauer et al., 2004a, 2004b). The overall wax components and cutin monomer ratios were similar, although overall cutin levels almost doubled in DFD fruits during ripening and were almost twice those of AC at the RR stage. No direct conclusions can be drawn from these results because the biochemical composition of tomato fruit cuticles varies among cultivars (Baker et al., 1982; Bauer et al., 2004a, 2004b) and the DFD trait is not available in an isogenic background for comparison with a wild type. Nevertheless, levels of cutin monomers are relatively constant among tomato cultivars with a range of morphological phenotypes and at different ripening stages (Baker et al., 1982; M. Jenks, T. Isaacson, and J. Rose, unpublished data) and we are not aware of any previous report that has described such high cutin levels, or the up-regulation of the cutin synthesis pathway during ripening. Moreover, the absence of a statistically significant increase in DFD cuticle thickness during ripening suggests that packing of the cutin matrix is much denser during ripening in DFD. The tomato fruit cutin matrix also becomes more cross-linked during ripening (Benítez et al., 2004) and so these two phenomena likely result in a stronger and less permeable cuticle membrane. Another important role of the cuticle is to provide a structural barrier against microbial pathogens (Mendgen et al., 1996) and many fungi secret cutinases to aid infection. The altered cutin profile of DFD, possibly associated with increased cutin cross-linking, might be connected to the observation that the fruits are highly resistant to microbial pathogens, unless the cuticle is damaged (Fig. 9).

CONCLUSION

DFD is unlike previously reported tomato mutants in that loss of fruit firmness is largely uncoupled from other aspects of ripening, thus providing a unique opportunity to examine the factors that contribute to fruit softening. Our results suggest that multiple coordinated processes are involved, including disassembly of polysaccharide networks in the primary wall and middle lamella and transpirational water/turgor loss. The minimal water loss and maintenance of cellular turgor in DFD fruit further allow an assessment of the relative contribution and timing of these two processes. In this regard, the turgor and fruit firmness data indicate that softening of intact fruits results from an early decline in cellular turgor coincident with early changes in wall architecture, presumably as a result of wall relaxation. A second component is then provided by substantial water transpiration, which occurs in parallel with continued wall degradation and a reduction in intercellular adhesion.

The cuticle itself is also thought to have an important influence on the biomechanical properties of ripening fruit (Petracek and Bukovac, 1995; Bargel and Neinhuis, 2004; Matas et al., 2004; Bargel and Neinhuis, 2005; Edelmann et al., 2005) and studies with isolated tomato fruit cuticles (Bargel and Neinhuis, 2005) suggest that their relative contribution to tissue strength increases markedly during ripening, an idea that was previously suggested by analyses of intact tomato fruits (Jackman and Stanley, 1994). Taken together, a growing body of evidence suggests that, as with cell wall metabolism, dynamic changes in the structure and composition of the fruit cuticle that lead to a reduction in fruit firmness are likely to be an integral and regulated part of ripening. The influence of the cuticle on fruit firmness would be both direct, acting as a load bearing matrix under tension, and indirect by regulating fruit water status. We note that our conclusions are based exclusively on studies with tomato and do not necessarily apply to all fruits.

While the goal of this study was not to identify the components of the cuticle that are responsible for

water permeance, DFD provides a valuable experimental system to address this question. Two features of DFD cuticle composition are particularly noteworthy and may provide some indication as the basis for the drastically reduced water permeance. First, the cutin matrix appears to be substantially denser and the consequent change in cuticle architecture and macromolecular packing may influence water permeability. Second, while the cuticles of most ripe tomatoes contain high levels of the flavonoid precursor naringenin chalcone (Bauer et al., 2004b), this compound was undetectable in DFD cuticles, which were therefore colorless. It has been suggested that this molecule can influence water permeability through the cuticle (Luque et al., 1995), although this has yet to be confirmed. Interestingly, it was recently reported that the cuticle of the nonripening *nor* mutant has a similar colorless phenotype (Bargel and Neinhuis, 2004), which we have confirmed, although cuticles of another pleiotropic nonripening mutant, *rin*, accumulated normal levels of naringenin chalcone (data not shown).

DFD is of obvious interest for agricultural biotechnology, a field that has to date focused almost exclusively on cell wall metabolism in an attempt to alter fruit softening and prolong shelf life. Our study reveals the clear distinction between complex textural changes in the pericarp flesh (sometimes called softening), which would be directly affected by wall metabolism, and the reduction in firmness of intact fruits, which is influenced by multiple factors, including the cuticle. The lack of progress in extending intact fruit firmness and quality by primarily targeting wall metabolism may partly reflect an underappreciation of this difference. Future research will be directed toward identifying the molecular elements that underlie the drastic reduction in water loss and apparently provide resistance to postharvest pathogens. Preliminary genetic analysis using a *Solanum pimpinellifolium* mapping population has revealed the existence of a single genetic locus that makes a major contribution to the DFD trait (data not shown) and the functional characterization of a candidate gene that cosegregates with that locus is currently in progress. In addition, as a control, the DFD trait is being introgressed into AC for further detailed phenotypic characterization.

MATERIALS AND METHODS

Plant Materials

Tomato fruit (*Solanum lycopersicum*; AC and DFD) plants were greenhouse grown at Cornell under 16 h light, 8 h dark conditions, using standard practices. Fruits were harvested at the following stages: MG, Br, turning, pink (Pi), light red, and RR based on external color, as described in Lashbrook et al. (1994). Fruits were designated as OR 1 week after reaching the RR stage. Flowers were tagged on the day of anthesis to monitor the developmental time course for each tomato cultivar. For the cellular turgor analyses plants were similarly grown and staged in the greenhouse in Davis, California. Fruits at the RR stage were stored at room temperature and ambient humidity or at high humidity in a sealed container for the microbial infection experiments. For the physiological and microbial infection studies, fruits were harvested at the appropriate stage immediately prior to analysis. For gene expression analysis, pericarp tissue was isolated at different stages and frozen immediately in liquid nitrogen and then stored at −80°C.

Respiration Rate and Ethylene Production Measurements

Six AC and DFD fruits were harvested at the MG stage and kept at 20°C. CO_2 and ethylene production of each fruit was measured by sealing individual fruit of known weight for 2 h in 475 mL glass jars fitted with sampling septa, on a daily basis for 9 or 21 d for AC or DFD, respectively. CO_2 concentrations in 1 mL samples of the headspace of each jar were measured using a Fisher Gas Partitioner (model 1200) gas chromatograph (GC; Fisher Scientific) equipped with a thermal conductivity detector. Ethylene concentrations were measured using a Hewlett-Packard 5710A GC (Hewlett-Packard) equipped with a flame ionization detector. Fruit color was measured using a Minolta CR300 color meter (Konica Minolta), expressing color change using the a* chromaticity coordinate.

Textural Analysis

Firmness measurements were made, based on compression of AC and DFD intact fruits (minimum of five replicate fruits), at MG, Br, Pi, RR, and RR plus 2 or 8 months. Each fruit was tested four times at equidistant points along the equatorial plane of the fruit with a 50 mm wide P50 DIA compression plate controlled by a Stable Microsystems Texture Analyzer (TA-XT2i; Stable Micro Systems), loading at 1 mm s^{-1} and compressed to a vertical displacement of 1 mm. Firmness was defined as the response force to a 0.05 N applied force. Fruits at the RR stage were detached, stored at room temperature, and analyzed after 60, 90, and 120 d for DFD and after 60 d for AC. To compare flesh firmness with compression of whole fruits, pericarp discs (1.5 cm diameter) were excised from the same fruit set with a cork borer and placed cuticle face up and tested as above. To determine the maximum force required to perforate the cuticle, segments of tomato pericarp were placed cuticle face down on a base plate with a vertical groove (3 mm wide) and the 1 mm probe applied until the cuticle was penetrated (40 replicates for each fruit stage). Statistical analysis was performed using SAS software (SAS Institute) and the Tukey-Kramer multiple comparison test.

The time-lapse video (Supplemental Video S1) was generated by taking a digital photograph (0.25 s exposure) of two AC fruits and one DFD fruit harvested at the MG stage and left to ripen at room temperature, every 10 min for approximately 4 months. Images were edited and compressed using Avid Xpress video editing software (Avid Technology).

Cell Wall Analysis

Cell walls were prepared from 50 g of diced outer pericarp of AC and DFD fruit (MG and RR stages) by boiling the pericarp pieces in 95% ethanol for 30 min to prevent autolytic activity, as described in Huysamer et al. (1997). Subsequent steps in preparing crude cell wall samples (alcohol-insoluble solids [AISs]) were also as in Huysamer et al. (1997), ending with two washes of the wall pellets with acetone and drying in a vacuum oven. Starch was removed by incubating 200 mg of AIS with 40 units each of α-amylase (from porcine pancreas, Sigma-Aldrich) and pullulanase (from *Bacillus acidopullulyticus*, Novozymes Biologicals) in 20 mL of Tris-HCl pH 7.0, 0.1% NaN_3, for 24 h. Neutral sugar composition of the AIS was determined by gas-liquid chromatography as in Campbell et al. (1990). Duplicate 2 to 3 mg samples of AIS were hydrolyzed in trifluoroacetic acid (TFA) and the TFA-soluble faction converted to alditol acetates and analyzed by gas-liquid chromatography (as in Rose et al., 1998). To measure the cellulose content of the AIS, the TFA-insoluble residues were dissolved in 67% H_2SO_4 and assayed using the anthrone reagent (Dische, 1962) with cellulose powder as a standard. Total uronic acids were determined using duplicate samples of the AIS with the Blumenkrantz and Asboe-Hansen (1973) assay, as modified by Ahmed and Labavitch (1977).

For the SEC analysis the AIS was treated with water and 50 mM cyclohexane diamine tetraacetic acid (CDTA; Rose et al., 1998). The water and CDTA-soluble materials (3–4 mg) were dissolved in 50 mM ammonium formate, pH 5 (500 μL), centrifuged to remove insoluble material and the soluble material analyzed by size-exclusion chromatography using a Superose-12 HR10/30 column (GE Healthcare). The column was eluted at 0.6 mL min^{-1} with 50 mM ammonium formate, pH 5, using a Dionex BioLc (Dionex). The eluant was monitored with a Knauer differential refractometer.

RNA Isolation and Analysis

Total RNA was isolated from pericarp fruit tissues as described in Wan and Wilkins (1994). A total of 15 μg per sample was subjected to electrophoresis on 1.2% agarose, 10% formaldehyde gels, and transferred to Hybond-N membranes (GE Healthcare) as described in Rose et al. (1997). Blots were hybridized at 42°C in 50% formamide, 6× sodium chloride/sodium phosphate/EDTA, 0.5% (w/v) SDS, 5× Denhardt's solution, and 100 mg mL^{-1} sheared salmon sperm DNA, with radiolabeled cDNA probes ([α-^{32}P]labeled cDNA) corresponding to the ripening-related genes *LeExp1* and *SlXTH5* (see Saladié et al., 2006), *LeExp3* (probe as described in Brummell et al., 1999), and *LePG1* (corresponding to the full length of GenBank accession CAA32235). cDNAs were generated with the Ready-To-Go DNA labeling beads ([α-^{32}P]dCTP) kit and ProbeQuant G-50 micro columns (GE Healthcare). Following hybridization, the membranes were washed three times in 5× SSC, 1% (w/v) SDS at 42°C for 15 min, followed by three washes in 0.2× SSC, 0.5% SDS at 65°C for 20 min.

Microscopy

Prior to microscopy pericarp thickness of AC and DFD fruits (15 replicates) was measured with calipers. To evaluate the pericarp cell size differences, pericarp from MG and RR stages were hand sectioned and viewed with a light microscope. Cell areas in the outer, middle, and inner pericarp zones (see Fig. 5) were calculated and statistical analyses performed using Image-Pro Plus software (Media Cybernetics).

For light microscopy visualization of cuticles, cuticular membranes were peeled from the fruits and fixed in formaldehyde:acetic acid 1:1 (v/v) in 18 volumes of 70% alcohol (formaldehyde-acetic acid) for 48 h, followed by dehydration in an alcohol series (50%–10%) and a water wash. Cuticle samples were frozen at −35°C and 10 μm sections were cut with a microtome and stained with 0.05% of toluidine blue. For TEM analysis of cuticles and cell separation, pericarp from AC and DFD RR fruits was excised from three replicate fruits at the equator at the RR stage and fixed for 1 h at room temperature in primary fixative, containing 2.5% (v/v) glutaraldehyde and 2% (v/v) formaldehyde in 0.05 M phosphate buffer (PB), pH 6.8 (Karnovsky, 1965). Sections were washed with PB and postfixed for 1 h in 2% (v/v) osmium tetroxide in 0.05 M PB. After washing with PB, the tissue slices were dehydrated through a gradient series of ethanol, infiltrated with Spurr's embedding medium (Electron Microscopy Science), and polymerized for 48 h at 60°C. Ultrathin (80–100 nm) sections were prepared from Spurr's resin-embedded samples and mounted on carbon-coated Formvar 100-mesh copper grids (Electron Microscopy Science). Sections were air dried, stained at room temperature with 2% (v/v) uranyl acetate for 5 min, and then with lead citrate for 3 min prior to viewing with a Philips EM 400 electron microscope (FEI company). Thick sections were also viewed using light microscopy.

For scanning electron microscopy analysis, pericarp from AC and DFD RR fruits was freeze dried in a VirTis Freeze mobile (VirTis Company) at −40°C, mounted on aluminum stubs, and sputter coated with gold/palladium using a BalTec SCD 050 coater (Balzers Union). Microscopic observations were made with a Hitachi S4500 scanning electron microscope (Hitachi High Technologies). Images were acquired using Princeton Gamma Tech Imix software (Princeton Gamma-Tech Instruments).

Turgor Analysis

Measurements of the turgor pressure of outer pericarp cells from detached intact AC and DFD fruits during ripening were performed as described in Shackel et al. (1991) by inserting a glass microcapillary into the pericarp cells located approximately 200 μm below the epidermal surface of intact fruits (Fig. 6A, inset), monitoring the probe location through a vertically illuminated microscope. Fruit ripening stage was evaluated by measuring external color at the equator point using a Minolta CR300 reflectance colorimeter to determine the a*, or red green, component of the L*a*b* uniform color space. Values for the MG, Br, RR, and OR stages corresponded to a* values of approximately −7 to −3, 5 to 6, 14 to 16, and ≥20, respectively.

Water Loss Measurements

Ten fruits from AC and DFD were detached at the RR stage and kept at room temperature for 3 months. Water loss per unit fruit surface area was calculated after measuring the weight decrease over time and measuring fruit dimensions.

Biomechanical Analysis of Cuticles

Rectangular strips of cuticle were removed from MG and RR AC, and DFD fruits using two parallel razor blades bonded to a metal block to give uniform segments with a width of 6.25 mm and incubated in a mixture of cellulase and pectinase (0.2% m/v and 20% m/v, respectively; Sigma) in sodium citrate buffer (50 mM, pH 4.0), 1 mM NaN_3 for 7 to 10 d at 37°C, followed by washes in sodium citrate buffer and dried at room temperature. A minimum of eight samples from each ripening stage was tested in unaxial tension using a model 4502 Instron Testing machine (Instron) and a 2.0 mm s^{-1} strain rate (see Matas et al., 2004). Data were rejected from samples that broke near or at their clamped ends; visual inspection of specimens during testing and of the shape of force-deformation graphs was used to assess clamp failure. From the tensile test, the breaking stress and the breaking strain were derived from stress-strain curves. Tensile stresses were calculated after the cross-sectional areas of mechanically tested samples were assessed using light microscope images and ImageJ image analysis software (http://rsb.info.nih.gov/ij) to determine the thickness of each sample. The exposed length of each sample was measured before extension with a hand-held microcaliper to determine tensile strains. All biomechanical analyses were performed in an air-conditioned laboratory and thus at constant temperature (24°C) and humidity since these factors can influence the cuticle biomechanical properties.

Cutin Monomer Analysis

Cuticles were enzymatically isolated (Schönherr and Riederer, 1986) from tomato fruit pericarp discs of known area incubated at 30°C in 20 mM citric acid, pH 3.7, containing 0.001% (w/v) phenylmercuric nitrate to prevent microbial growth. After 72 h cuticles were washed in an acetone series and refluxed for 24 h in a Soxhlet apparatus with chloroform:methanol (1:1) and 50 mg L^{-1} butylated hydroxytoluene. After washing with methanol to remove chloroform, the cuticles were depolymerized in 8 mL anhydrous methanol containing 7.5% (v/v) methyl acetate and 4.5% (w/v) sodium methoxide at 60°C (Bonaventure et al., 2004). Methyl heptadecanoate and ω-pentadecalactone were added as internal standards. After 16 h the reaction was cooled, adjusted to pH 4 to 5 with acetic acid, followed by two dichloromethane extractions (10 mL) to remove methyl ester monomers (Bonaventure et al., 2004). The organic phase was washed three times with 0.9% NaCl (w/v), dried with 2,2-dimethoxypropane, and dried under nitrogen gas. Monomers were derivatized by reaction for 15 min at 100°C with pyridine:N,O,-bis(trimethylsilyl)-trifluoroacetamide (BSTFA; 1:1). The excess pyridine:BSTFA was removed with nitrogen gas, and the sample dissolved in heptane:toluene (1:1) prior to analysis with a Hewlett-Packard 5890 series II GC equipped with a flame ionization detector and 12 m, 0.2 mm id HP-1 capillary column with helium as the carrier gas. The GC was programmed with an initial temperature of 80°C and increased at 15°C min^{-1} to 200°C, then increased at 2°C min^{-1} to 280°C. Quantification was based on flame ionization detector peak areas and internal standard methyl heptadecanoate. Specific correction factors were developed from multilevel calibration curves (as for wax analysis, Jenks et al., 1995) developed from external standards hexadecanoic acid, hexadecane-1,16-dioic acid, 16-hydroxy hexadecanoic acid, and octadecanoic acid (Aldrich). All values shown in tables represent the average of three replicate samples. Selected subsamples were analyzed in a GC-mass spectrometer (FinniganMAT/Thermospray Corporation) to confirm the identities of some derivatives.

All cutin monomers were identified from electron impact mass spectrometry of the methyl ester trimethylsilyl derivatives on the basis of the published spectra (Eglinton and Hunneman, 1968; Holloway, 1982), retention indexes (Holloway, 1984), and retention times of the authentic standards hexadecanoic acid, hexadecane-1,16-dioic acid, 16-hydroxy hexadecanoic acid, and octadecanoic acid.

Cuticular Wax Analysis

Based on Jenks et al. (1995), the chloroform-soluble cuticular wax extracts from tomato pericarp samples of known area were evaporated to dryness under a stream of nitrogen gas and the dried residue prepared for GC by derivatization using BSTFA. Extracts were derivatized for 15 min at 100°C. After evaporation of excess BSTFA under nitrogen, the samples were redissolved in hexane for GC analysis with a Hewlett-Packard 5890 series II GC, equipped with a flame ionization detector and a 12 m, 0.2 mm HP-1 capillary column with helium as the carrier gas. The GC was programmed with an initial temperature of 80°C and increased at 15°C min^{-1} to 260°C, where the

temperature remained unchanged for 10 min. The temperature was then increased at 5°C min^{-1} to 320°C, then held for 15 min. Quantification was based on flame ionization detector peak areas and the internal standard hexadecane. Specific correction factors were developed from external standards and applied to the peak areas of the free fatty acids, saturated primary alcohols, and odd chain-length *n*-alkanes. For all other peaks, a factor of 1.03 was assigned (the average correction for external standards at comparable concentrations). The total amount of cuticular wax was expressed per pericarp area as determined by measuring scanned pericarp areas using Image J 1.32j (National Institutes of Health). All values represent the average of three replicate plant samples. Selected subsamples were analyzed by GC-mass spectrometry. Because tritriacontane and δ-amyrin coeluted during the above GC analysis, an additional GC analysis was performed for each sample using a temperature program to separate these constituents. The GC was programmed with an initial temperature of 80°C and increased at 15°C min^{-1} to 220°C, held for 65 min, then increased 15°C min^{-1} to 320°C, then for held 10 min. A ratio was calculated for tritriacontane and δ-amyrin to determine the amount of tritriacontane and δ-amyrin.

GC-Mass Spectrometry Analysis of Flavonoids

Lipophillic components were determined following minor modification to the method described by Fiehn et al. (2000). For metabolite analysis mass spectral peaks were compared to mass spectral libraries in the Golm Metabolome Database (Kopka et al., 2005; Schauer et al., 2005).

Microbial Inoculation and Infection

Fruits from AC and DFD at the RR stage were stored at room temperature in a moist container to assess opportunistic microbial infection. RR fruits from DFD, AC, and a commercially purchased cultivar were inoculated with three concentrations of *Botrytis cinerea* (strain Del 11) spores (10^3, 10^6, and 10^8) by ectopic application onto the fruit surface or by injecting immediately underneath the cuticle surface. Fruits were stored in moist sealed boxes at room temperature.

Statistical Analyses

All statistical analyses were performed using the JMP software package (SAS Institute). All comparisons among means (*t* test; $\alpha = 0.05$) were used to determine differences between the cultivars (see figure legends for each *n* value). Data are presented as means and the SE with a level of significance of 5% ($P = 0.05$), unless otherwise other noted.

Supplemental Data

The following materials are available in the online version of this article.

Supplemental Figure S1. Microscopy analysis of tomato fruit pericarp cell separation.

Supplemental Video S1. A time-lapse video spanning 4 months showing two AC fruits (left and right) and one DFD fruit (middle) during storage at ambient temperature and humidity.

ACKNOWLEDGMENTS

We thank Yonghua He and Carl Greve (fruit staging and analysis), Randy Wayne and Dominick Paolillo (light microscopy), Hamid Ahmadi (turgor pressure), Kent Loeffler (photography), Stefan Einarson (time-lapse photography), Christopher Hogan (Instron evaluation), David Kidd (textural analysis), and Jackie Nock (ethylene and carbon dioxide measurements). We also thank Josep Saladié and Ann Powell for providing seeds and *B. cinerea* cultures, respectively, and we are grateful to Antonio Heredia, Jim Giovannoni, and Steve Tanksley for helpful advice and discussion.

Received February 2, 2007; accepted April 12, 2007; published April 20, 2007.

LITERATURE CITED

Ahmed AER, Labavitch JM (1977) A simplified method for accurate determination of cell wall uronic acid content. J Food Biochem **1:** 361–365

Almeida DPF, Huber DJ (1999) Apoplastic pH and inorganic ion levels in tomato fruit: a potential means for regulation of cell wall metabolism during ripening. Physiol Plant **105:** 506–512

Baker EA, Bukovac MJ, Hunt GM (1982) Composition of tomato fruit cuticle as related to fruit growth and development. *In* DF Cutler, KL Alvin, CE Price, eds, The Plant Cuticle. Academic Press, London, pp 33–44

Banik M, Bourgault R, Bewley JD (2001) Endo-β-mannanase is present in an inactive form in ripening tomato fruits of the cultivar Walter. J Exp Bot **52:** 105–111

Bargel H, Neinhuis C (2004) Altered tomato (*Lycopersicon esculentum* Mill.) fruit cuticle biomechanics of a pleiotropic non ripening mutant. J Plant Growth Regul **23:** 61–75

Bargel H, Neinhuis C (2005) Tomato (*Lycopersicon esculentum* Mill.) fruit growth and ripening as related to the biomechanical properties of fruit skin and isolated cuticle. J Exp Bot **56:** 1049–1060

Barrett DM, Garcia E, Wayne JE (1998) Textural modification of processing tomatoes. Crit Rev Food Sci Nutr **38:** 173–258

Bauer S, Schulte E, Thier HP (2004a) Composition of the surface wax from tomatoes. I. Identification of the components by GC/MS. Eur Food Res Technol **219:** 223–228

Bauer S, Schulte E, Thier HP (2004b) Composition of the surface wax from tomatoes. II. Quantification of the components at the ripe red stage and during ripening. Eur Food Res Technol **219:** 487–491

Benítez JJ, Matas AJ, Heredia A (2004) Molecular characterization of the plant biopolyester cutin by AFM and spectroscopic techniques. J Struct Biol **147:** 179–184

Blumenkrantz N, Asboe-Hansen G (1973) New method for quantitative-determination of uronic acids. Anal Biochem **54:** 484–489

Blumer JM, Clay RP, Bergmann CW, Albersheim P, Darvill A (2000) Characterization of changes in pectin methylesterase expression and pectin esterification during tomato fruit ripening. Can J Bot **78:** 607–618

Bonaventure G, Beisson F, Ohlrogge J, Pollard M (2004) Analysis of the aliphatic monomer composition of polyesters associated with Arabidopsis epidermis: occurrence of octadeca-cis-6, cis-9-diene-1,18-dioate as the major component. Plant J **40:** 920–930

Brownleader MD, Jackson P, Mobasheri A, Pantelides AT, Sumar S, Trevan M, Dey PM (1999) Molecular aspects of cell wall modifications during fruit ripening. Crit Rev Food Sci Nutr **39:** 149–164

Brummell DA (2006) Cell wall disassembly in ripening fruit. Funct Plant Biol **33:** 103–119

Brummell DA, Harpster MH (2001) Cell wall metabolism in fruit softening and quality and its manipulation in transgenic plants. Plant Mol Biol **47:** 311–340

Brummell DA, Harpster MH, Dunsmuir P (1999) Differential expression of expansin gene family members during growth and ripening of tomato fruit. Plant Mol Biol **39:** 161–169

Burghardt M, Riederer M (2006) Cuticular transpiration. *In* M Riederer, C Müller, eds, Biology of the Plant Cuticle: Annual Plant Reviews Series, Vol 23. Blackwell Publishing Ltd., Oxford, pp 292–311

Cameron AC, Yang SF (1982) A simple method for the determination of resistance to gas-diffusion in plant organs. Plant Physiol **70:** 21–23

Campbell AD, Huysamer M, Stotz HU, Greve LC, Labavitch JM (1990) Comparison of ripening processes in intact tomato fruit and excised pericarp disks. Plant Physiol **94:** 1582–1589

Carey AT, Holt K, Picard S, Wilde R, Tucker GA, Bird CR, Schuch W, Seymour GB (1995) Tomato exo-(1 → 4)-β-*D*-galactanase: isolation, changes during ripening in normal and mutant tomato fruit, and characterization of a related cDNA clone. Plant Physiol **108:** 1099–1107

Casado CG, Heredia A (2001) Self-association of plant wax components: a thermodynamic analysis. Biomacromolecules **2:** 407–409

Cosgrove DJ (1993) Wall extensibility—its nature, measurement and relationship to plant-cell growth. New Phytol **124:** 1–23

Davuluri GR, van Tuinen A, Fraser PD, Manfredonia A, Newman R, Burgess D, Brummell DA, King SR, Palys J, Uhlig J, et al (2005) Fruit-specific RNAi-mediated suppression of *DET1* enhances carotenoid and flavonoid content in tomatoes. Nat Biotechnol **23:** 890–895

Dharmapuri S, Rosati C, Pallara P, Aquilani R, Bouvier F, Camara B, Giuliano G (2002) Metabolic engineering of xanthophyll content in tomato fruits. FEBS Lett **519:** 30–34

Dische Z (1962) Color reactions of carbohydrates. *In* RL Whistler, ML Wolfrom, eds, Methods in Carbohydrate Chemistry, Vol 1. Academic Press, New York, pp 477–512

Edelmann HG, Neinhuis C, Bargel H (2005) Influence of hydration and temperature on the rheological properties of plant cuticles and their impact on plant organ integrity. J Plant Growth Regul **24:** 116–126

Eglinton G, Hunneman DH (1968) Gas chromatographic-mass spectrometric studies of long chain hydroxy acids. I. Constituent cutin acids of apple cuticle. Phytochemistry **7:** 313–322

Eriksson EM, Bovy A, Manning K, Harrison L, Andrews J, De Silva J, Tucker GA, Seymour GB (2004) Effect of the *Colorless non-ripening* mutation on cell wall biochemistry and gene expression during tomato fruit development and ripening. Plant Physiol **136:** 4184–4197

Fiehn O, Kopka J, Trethewey RN, Willmitzer L (2000) Identification of uncommon plant metabolites based on calculation of elemental compositions using gas chromatography and quadrupole mass spectrometry. Anal Chem **72:** 3573–3580

Fraser PD, Bramley PM (2004) The biosynthesis and nutritional uses of carotenoids. Prog Lipid Res **43:** 228–265

Giovannoni JJ (2004) Genetic regulation of fruit development and ripening. Plant Cell **16:** S170–S180

Guillén F, Castillo S, Zapata PJ, Martínez-Romero D, Valero D, Serrano M (2006) Efficacy of 1-MCP treatment in tomato fruit 2: effect of cultivar and ripening stage at harvest. Postharvest Biol Technol **42:** 235–242

Harker FR, Redgwell RJ, Hallett IC, Murray SH, Carter G (1997) Texture of fresh fruit. Hortic Rev (Am Soc Hortic Sci) **20:** 121–124

Holloway PJ (1982) The chemical constitution of plant cutins. *In* DF Cutler, KL Alvin, CE Price, eds, The Plant Cuticle. Academic Press, London, pp 45–85

Holloway PJ (1984) Cutins and suberins, the polymeric plant lipids. *In* HK Mangold, G Zweig, J Sherma, eds, CRC Handbook of Chromatography: Lipids, Vol 1. CRC Press, Boca Raton, Florida, pp 321–345

Huysamer M, Greve LC, Labavitch JM (1997) Cell wall metabolism in ripening fruit. IX. Synthesis of pectic and hemicellulosic cell wall polymers in the outer pericarp of mature green tomatoes (cv XMT-22). Plant Physiol **114:** 1523–1531

Jackman RL, Marangoni AG, Stanley DW (1992) The effects of turgor pressure on puncture and viscoelastic properties of tomato tissue. J Texture Stud **23:** 491–505

Jackman RL, Stanley DW (1994) Influence of the skin on puncture properties of chilled and nonchilled tomato fruit. J Texture Stud **25:** 221–230

Jackman RL, Stanley DW (1995) Creep behaviour of tomato pericarp tissue as influenced by ambient temperature ripening and chilled storage. J Texture Stud **26:** 537–552

Jeffree CE (2006) The fine structure of the plant cuticle. *In* M Riederer, C Müller, eds, Biology of the Plant Cuticle Annual Plant Reviews Series, Vol 23. Blackwell Publishing Ltd., Oxford, pp 11–125

Jenks MA, Tuttle HA, Eigenbrode SD, Feldmann KA (1995) Leaf epicuticular waxes of the *Eceriferum* mutants in Arabidopsis. Plant Physiol **108:** 369–377

Jeong H, Huber DJ, Sargent SA (2003) Delay of avocado (*Persea americana*) fruit ripening by 1-methylcyclopropene and wax treatments. Postharvest Biol Technol **28:** 247–257

Karnovsky MJ (1965) A formaldehyde-glutaraldehyde fixative of high osmolality for use in electron microscopy. J Cell Biol **27:** A137

Klee HJ (1993) Ripening physiology of fruit from transgenic tomato (*Lycopersicon esculentum*) plants with reduced ethylene synthesis. Plant Physiol **102:** 911–916

Kopeliovitch E, Mizrahi Y, Rabinowitch HD, Kedar N (1980) Physiology of the tomato mutant *Alcobaca*. Physiol Plant **48:** 307–311

Kopka J, Schauer N, Krueger S, Birkemeyer C, Usadel B, Bergmuller E, Dormann P, Weckwerth W, Gibon Y, Stitt M, et al (2005) GMD@CSB.DB: the golm metabolome database. Bioinformatics (Oxf) **21:** 1635–1638

Lashbrook CC, Gonzalez-Bosch C, Bennett AB (1994) Two divergent endo-β-1,4-glucanase genes exhibit overlapping expression in ripening fruit and abscising flowers. Plant Cell **6:** 1485–1493

Lewinsohn E, Schalechet F, Wilkinson J, Matsui K, Tadmor Y, Nam KH, Amar O, Lastochkin E, Larkov O, Ravid U, et al (2001) Enhanced levels of the aroma and flavor compound S-linalool by metabolic engineering of the terpenoid pathway in tomato fruits. Plant Physiol **127:** 1256–1265

Lin TT, Pitt RE (1986) Rheology of apple and potato tissue as affected by cell turgor pressure. J Texture Stud **17:** 291–313

Lu C, Zainal Z, Tucker GA, Lycett GW (2001) Developmental abnormalities and reduced fruit softening in tomato plants expressing an antisense Rab11 GTPase gene. Plant Cell **13:** 1819–1833

Luque P, Bruque S, Heredia A (1995) Water permeability of isolated cuticular membranes—a structural-analysis. Arch Biochem Biophys **317:** 417–422

Maclachlan G, Brady C (1994) Endo-1,4-β-glucanase, xyloglucanase, and xyloglucan endo-transglycosylase activities versus potential substrates in ripening tomatoes. Plant Physiol **105:** 965–974

Matas AJ, Cobb ED, Bartsch JA, Paolillo DJ, Niklas KJ (2004) Biomechanics and anatomy of *Lycopersicon esculentum* fruit peels and enzyme-treated samples. Am J Bot **91:** 352–360

Mendgen K, Hahn M, Deising H (1996) Morphogenesis and mechanisms of penetration by plant pathogenic fungi. Annu Rev Phytopathol **34:** 367–386

Mignani I, Greve LC, Benarie R, Stotz HU, Li CY, Shackel KA, Labavitch JM (1995) The effects of GA(3) and divalent-cations on aspects of pectin metabolism and tissue softening in ripening tomato pericarp. Physiol Plant **93:** 108–115

Muir SR, Collins GJ, Robinson S, Hughes S, Bovy A, De Vos CHR, van Tunen AJ, Verhoeyen ME (2001) Overexpression of petunia chalcone isomerase in tomato results in fruit containing increased levels of flavonols. Nat Biotechnol **19:** 470–474

Mutschler MA (1984) Ripening and storage characteristics of the *Alcobaca* ripening mutant in tomato. J Am Soc Hortic Sci **109:** 504–507

Niklas KJ (1992) Plant Biomechanics: An Engineering Approach to Plant Form and Function. University of Chicago Press, Chicago

Orfila C, Huisman MMH, Willats WGT, van Alebeek G, Schols HA, Seymour GB, Knox JP (2002) Altered cell wall disassembly during ripening of *Cnr* tomato fruit: implications for cell adhesion and fruit softening. Planta **215:** 440–447

Petracek PD, Bukovac MJ (1995) Rheological properties of enzymatically isolated tomato fruit cuticle. Plant Physiol **109:** 675–679

Riederer M, Schreiber L (2001) Protecting against water loss: analysis of the barrier properties of plant cuticles. J Exp Bot **52:** 2023–2032

Romer S, Fraser PD, Kiano JW, Shipton CA, Misawa N, Schuch W, Bramley PM (2000) Elevation of the provitamin A content of transgenic tomato plants. Nat Biotechnol **18:** 666–669

Rose JKC, Catalá C, Gonzalez-Carranza CZH, Roberts JA (2003) Plant cell wall disassembly. *In* JKC Rose, ed, The Plant Cell Wall, Vol 8. Blackwell Publishing Ltd, Oxford, pp 264–324

Rose JKC, Hadfield KA, Labavitch JM, Bennett AB (1998) Temporal sequence of cell wall disassembly in rapidly ripening melon fruit. Plant Physiol **117:** 345–361

Rose JKC, Lee HH, Bennett AB (1997) Expression of a divergent expansin gene is fruit-specific and ripening-regulated. Proc Natl Acad Sci USA **94:** 5955–5960

Ruan YL, Patrick JW, Brady CJ (1996) The composition of apoplast fluid recovered from intact developing tomato fruit. Aust J Plant Physiol **23:** 9–13

Saladié M, Rose JKC, Cosgrove DJ, Catalá C (2006) Characterization of a new xyloglucan endotransglucosylase/hydrolase (XTH) from ripening tomato fruit and implications for the diverse modes of enzymic action. Plant J **47:** 282–295

Schauer N, Steinhauser D, Strelkov S, Schomburg D, Allison G, Moritz T, Lundgren K, Roessner-Tunali U, Forbes MG, Willmitzer L, et al (2005) GC-MS libraries for the rapid identification of metabolites in complex biological samples. FEBS Lett **579:** 1332–1337

Schönherr J, Riederer M (1986) Plant cuticles sorb lipophilic compounds during enzymatic isolation. Plant Cell Environ **9:** 459–466

Schreiber L (2005) Polar paths of diffusion across plant cuticles: new evidence for an old hypothesis. Ann Bot **95:** 1069–1073

Schreiber L (2006) Characterization of polar paths of transport in plant cuticles. *In* M Riederer, C Müller, eds, Biology of the Plant Cuticle: Annual Plant Reviews Series, Vol 23. Blackwell Publishing Ltd., Oxford, pp 280–291

Schuelter AR, Finger FL, Casali VWD, Brommonschenkel SH, Otoni WC (2002) Inheritance and genetic linkage analysis of a firm-ripening tomato mutant. Plant Breed **121:** 338–342

Seymour GB, Manning K, Eriksson EM, Popovich AH, King GJ (2002) Genetic identification and genomic organization of factors affecting fruit texture. J Exp Bot **53:** 2065–2071

Shackel KA, Greve C, Labavitch JM, Ahmadi H (1991) Cell turgor changes associated with ripening in tomato pericarp tissue. Plant Physiol **97:** 814–816

Thompson AJ, Tor M, Barry CS, Vrebalov J, Orfila C, Jarvis MC, Giovannoni JJ, Grierson D, Seymour GB (1999) Molecular and genetic characterization of a novel pleiotropic tomato-ripening mutant. Plant Physiol **120:** 383–389

Vega A, Luza J, Espina S, Lizana LA (1991) Characterization of the epidermis of three blueberry (*Vaccinium corymbosum* L.) cltivars and water loss at different storage temperatures. Proc Interamer Soc Tropic Hort **35:** 263–274

Waldron KW, Parker ML, Smith AC (2003) Plant cell walls and food quality. Comp Rev Food Sci Food Safety **2:** 101–119

Wallner SJ, Bloom HL (1977) Characteristics of tomato cell wall degradation in vitro: implications for the study of fruit-softening enzymes. Plant Physiol **60:** 207–210

Wan CY, Wilkins TA (1994) A modified hot borate method significantly enhances the yield of high-quality RNA from cotton (*Gossypium hirsutum* L). Anal Biochem **223:** 7–12